

The effect of intra- and interspecific competition on coexistence in multispecies communities

György Barabás, Matthew J. Michalska-Smith & Stefano Allesina

The American Naturalist (in press)

Abstract

For two competing species, intraspecific competition must exceed interspecific competition for coexistence. To generalize this well-known criterion to multiple competing species, one must take into account both the distribution of interaction strengths and community structure. Here we derive a multispecies generalization of the two-species rule in the context of symmetric Lotka–Volterra competition, and obtain explicit stability conditions for random competitive communities. We then explore the influence of community structure on coexistence. Results show that both the most and least stabilized cases have striking global structures, with a nested pattern emerging in both cases. The distribution of intraspecific coefficients leading to the most and least stabilized communities also follows a predictable pattern that can be justified analytically. In addition, we show that the size of the parameter space allowing for feasible communities always increases with the strength of intraspecific effects in a characteristic way that is independent of the interspecific interaction structure. We conclude by discussing possible extensions of our results to nonsymmetric competition.

Keywords: coexistence, community structure, interspecific competition, intraspecific competition, Lotka–Volterra model

1 Introduction

The familiar textbook statement, based on the analysis of two-species Lotka–Volterra competition, is that intraspecific competition must be greater than interspecific competition for two species to coexist (Case 2000, p. 331, Gotelli 2008, p. 104, Mittelbach 2012, p. 130, Vandermeer and Goldberg 2013, p. 208). This mathematical result formalizes the attractively simple intuition that species must limit themselves more than their competitors for coexistence (Chesson 2000): if any one of the species reaches high abundance, it must hinder itself more than its competitor, ensuring that neither can completely take over.

One important question is how this simple and well-known coexistence rule generalizes to multispecies communities. When more than two species compete, things quickly get very complicated, even in the context of the classic competitive Lotka–Volterra model (May and Leonard 1975, Case 2000, pp. 333–341). The difficulty is that community structure influences coexistence, but whereas two-species communities have a very simple structure, the same is not true of multispecies communities. Importantly, the two-species coexistence rule no longer holds. Indeed, it is possible to formulate even three-species scenarios where 1) every pair satisfies the rule, yet the

three species cannot coexist; and 2) the pairs violate the rule, yet the three species do coexist at a stable equilibrium (Appendix B, Section B2.3). Therefore, in larger systems the two-species condition is neither necessary nor sufficient: it is, in general, no condition for coexistence at all. This means that the original, straightforward two-species intuition is not quite so straightforward in multispecies communities. One cannot simply think of such systems as collections of pairwise interactions, so that every pair fulfilling the two-species coexistence condition would guarantee the dynamical stability of feasible equilibria (a “feasible equilibrium” is one where all species have positive abundances).

Techniques for evaluating the stability of multispecies communities have been available for many decades, and include invasion analysis, loop analysis, and qualitative modeling. Invasion analysis (Chesson and Ellner 1989, Chesson 1994, 2009, Adler et al. 2007, Siepielski and McPeck 2010) attempts to reduce the single, complicated problem of S competing species to S simple problems, where one species invades, from low abundance, the community formed by the other $S - 1$ species at the stationary state corresponding to the absence of the invader. The species are considered coexisting if each has positive growth when invading. This approach has generated great advances, both on the theoretical (Chesson 1994, 2000, Adler et al. 2007, Siepielski and McPeck 2010) and empirical (Levine and Rees 2004, Levine and HilleRisLambers 2009, Siepielski et al. 2010, Adler et al. 2010) side of community ecology. Unfortunately however, like any method, invasion analysis has its limitations. The outcome of invasion depends on the steady state of the $(S - 1)$ -species community where the invader is absent—however, obtaining this is often every bit as difficult as the original S -species problem, so nothing is gained. Also, there is no guarantee that in the absence of a single invader the rest of the community will not experience further extinctions, resulting in a state where the originally removed species cannot invade alone, but would be able to invade in concert with some other species (Case 1990, Law and Morton 1996, Edwards and Schreiber 2010). Invasibility can therefore be too strict a criterion, which might erroneously classify cases of true coexistence as mere co-occurrence, in the sense of Leibold and McPeck (2006).

Loop analysis and qualitative modeling (Levins 1968, May 1973, Levins 1974, 1975, Justus 2006) focus on evaluating the local stability of coexistence equilibria. Indeed, the two-species coexistence rule can be derived using loop analysis. The main limitation of these approaches is that results can typically be obtained only in cases where either the number of species is low, or the general structure of interactions especially simple (Justus 2006). The reason is that loop analysis is a “graphical translation” of the Routh-Hurwitz stability criteria (Edelstein-Keshet 1988): as the number of species increases, both the number and complexity of these criteria increase, and even if one were to evaluate them somehow, the results would lack the clear biological interpretation that is available in e.g. the two-species case in terms of the intra- and interspecific competition coefficients.

Here we ask what can be said about the relationship between intra- and interspecific competition and coexistence in multispecies competitive communities, and how community structure affects this relationship in the context of Lotka–Volterra competition. Due to the aforementioned difficulties with classical methods of analysis, our strategy is instead to decompose the interaction matrix as the sum of an intra- and an interspecific part, and to study the dynamical stability of coexistence via the eigenvalues of these parts. We restrict most of our analyses to symmetric competition, commenting on the more general case in Appendix A (“The case of nonsymmetric interaction matrices”) and the Discussion. Symmetric interaction matrices naturally arise in many competition models, e.g., in those based on niche overlap (MacArthur and Levins 1967, Levins 1968, MacArthur

1972, Roughgarden 1979, Case 2000, Hernández-García et al. 2009). Also, symmetry allows for a clear disentangling of the problems of stability and feasibility, makes local stability properties reflect global stability, and offers a way of relating intra- to interspecific competition not available in the nonsymmetric case.

This work is structured as follows. After reviewing our methods, we present simple analytical results extending the two-species coexistence rule to the multispecies case. Next, we relate the effect of community structure on intra- and interspecific competition and community stability, using random communities as our baseline (i.e., with competition coefficients randomly and independently sampled). We find that both the most and least stabilized communities possess simple, characteristic structures that can be interpreted biologically. Additionally, since an equilibrium needs to be both stable and feasible to describe coexistence (Mészéna et al. 2006, Barabás et al. 2012, Rohr et al. 2014, Grilli et al. 2015), we explore the influence of community structure on feasibility as well as stability. We conclude by discussing possible extensions of our results to the case of nonsymmetric competition.

2 Methods

We start from the generalized Lotka–Volterra equations for S species:

$$\frac{d\mathbf{n}}{dt} = \text{diag}(\mathbf{n})(\mathbf{b} + \mathbf{A}\mathbf{n}) \quad (1)$$

(Appendix B, Section B2.1), where t is time, \mathbf{n} is the vector of species densities, $\text{diag}(\mathbf{n})$ is the $S \times S$ matrix with the entries of \mathbf{n} along its diagonal and zeros elsewhere, \mathbf{b} is the vector of intrinsic growth rates, and \mathbf{A} is the interaction matrix; its (i, j) th entry is the amount of change in species i 's per capita growth rate caused by a unit increase in species j 's density.

We wish to study the stability and feasibility of coexistence generated by Eq. (1) in light of the distribution of intra- and interspecific interaction strengths. To disentangle the effects of the two, we write $\mathbf{A} = \mathbf{B} + \mathbf{C}$, where \mathbf{B} only contains interspecific and \mathbf{C} only intraspecific effects; therefore \mathbf{B} is equal to \mathbf{A} except it has zeros along its diagonal, and \mathbf{C} contains only the diagonal entries of \mathbf{A} with all offdiagonal entries being zero. We denote the (i, j) th entries of these matrices by A_{ij} , B_{ij} , and C_{ij} , respectively; since we are concerned with competition, all coefficients are nonpositive.

For \mathbf{A} symmetric, its rightmost eigenvalue being less than zero guarantees the global stability of coexistence in the Lotka–Volterra model, provided the coexistence equilibrium is feasible (Appendix B, Section B2.1). This greatly simplifies stability analysis by obviating the need to evaluate the Jacobian at equilibrium. Also, since \mathbf{A} , \mathbf{B} , and \mathbf{C} are all symmetric, their eigenvalues are real, so they can be numbered in decreasing order. Let the eigenvalues of \mathbf{A} be $\alpha_1 \geq \alpha_2 \geq \dots \geq \alpha_S$, those of \mathbf{B} $\beta_1 \geq \beta_2 \geq \dots \geq \beta_S$, and those of \mathbf{C} $\gamma_1 \geq \gamma_2 \geq \dots \geq \gamma_S$. Note that, since \mathbf{C} is a diagonal matrix, its eigenvalues are the diagonal entries themselves. Therefore $\gamma_1 = \max A_{ii} = \max C_{ii}$ is the weakest and $\gamma_S = \min A_{ii} = \min C_{ii}$ is the strongest intraspecific competition coefficient.

Moreover, the symmetry of \mathbf{B} and \mathbf{C} allows one to derive further conditions on \mathbf{A} 's stability. From Weyl's inequality (Fulton 2000), we have, respectively, the necessary and sufficient conditions

$$\beta_1 + \gamma_S < 0, \quad \beta_1 + \gamma_1 < 0 \quad (2)$$

for the stability of \mathbf{A} (Appendix B, Section B3). In words, the strongest intraspecific interaction being able to offset the interspecific effects is a necessary condition, while the weakest intraspecific

interaction being able to offset the interspecific effects is a sufficient condition for the stability of \mathbf{A} . If all intraspecific coefficients are equal, then $\gamma_1 = \gamma_S$ and the two conditions are equivalent, providing a necessary and sufficient condition for stability. In case the intraspecific coefficients are not equal (the most general situation), fulfilling the sufficient condition $\beta_1 + \gamma_1 < 0$ guarantees stability.

Since the rightmost eigenvalue β_1 of \mathbf{B} appears in both conditions, it is obviously important for the stability of coexistence. We are therefore interested in how community structure influences β_1 . To study this question, we first generate \mathbf{B} by sampling its entries randomly—this ensures that any resulting community structure is coincidental. Then, using a genetic algorithm (Appendix B, Section B5), we rearrange \mathbf{B} 's entries to minimize/maximize β_1 , and analyze the structure of the resulting matrices. In other words, we keep the same set of entries but, preserving the symmetry of \mathbf{B} , assign them to different species pairs such that the community composition becomes easier/more difficult to stabilize than if we were to shuffle the interaction strengths at random. The minimum possible β_1 corresponds to the most stabilized, while the maximum β_1 to the least stabilized community.

Turning to the matrix \mathbf{C} of intraspecific coefficients, we ask the same question: how should they be distributed across species to minimize/maximize the rightmost eigenvalue of \mathbf{A} ; i.e., to lead to the most and least stabilized communities? Since the answer depends on the arrangement of the coefficients of \mathbf{B} , we perform the optimization of \mathbf{C} (using the same method as for \mathbf{B}) for all three cases: \mathbf{B} arranged to minimize β_1 , \mathbf{B} random, and \mathbf{B} arranged to maximize β_1 .

Finally, we investigate the feasibility of the coexistence, i.e., determine when are all equilibrium densities strictly positive. The only equilibrium solution of Eq. (1) where all species may coexist is $\mathbf{n} = -\mathbf{A}^{-1}\mathbf{b}$, so for a given matrix \mathbf{A} we can determine which vectors \mathbf{b} make this product all-positive. Note that if $\mathbf{n} = -\mathbf{A}^{-1}\mathbf{b}$ is feasible for some \mathbf{b} , then it is also feasible for $\eta\mathbf{b}$ with η an arbitrary positive constant, since this will lead to $-\mathbf{A}^{-1}(\eta\mathbf{b}) = \eta\mathbf{n}$ as the new equilibrium solution. Therefore, the magnitude of \mathbf{b} is inconsequential for feasibility; only its direction matters. Using an appropriate integral formula (Appendix B, Section B7), we numerically determine the ratio of feasible to nonfeasible directions of the vector \mathbf{b} .

3 Interspecific competition and community stability

3.1 A simple multispecies generalization of the two-species coexistence rule

For two competing species, stability of the coexistence equilibrium $\mathbf{n} = -\mathbf{A}^{-1}\mathbf{b}$ of Eq. (1) is achieved if $A_{11}A_{22} > A_{12}A_{21}$, meaning that the geometric mean of the intraspecific competition coefficients has to exceed the geometric mean of the interspecific ones (Appendix B, Section B2.2; note that this two-species coexistence rule only guarantees stability, but not feasibility). What happens when the number of species is greater than two? We have seen that Weyl's inequality provides necessary and sufficient stability criteria if \mathbf{A} is symmetric. In that case however, there also exists a more direct multispecies generalization. The result, based on a simple corollary of Sylvester's criterion (Appendix B, Section B2.5), is that for stability, all species pairs must individually satisfy the two-species coexistence rule. This condition is necessary but not sufficient, i.e., violating it guarantees instability, but fulfilling it does not guarantee stability.

3.2 Random interspecific interaction matrices

To study the effect of community structure on stability, let us start from a randomly assembled $S \times S$ interaction matrix. In particular: the matrix \mathbf{B} of interspecific coefficients has zeros along the diagonal, every entry in the upper triangle is drawn independently from some distribution with mean $\mu < 0$ and variance V , and the lower triangle is filled out to make \mathbf{B} symmetric. A similar approach has been followed for studying the stability of replicator dynamics; see Diederich and Oppen (1989) in the context of symmetric payoff matrices, and Oppen and Diederich (1992) and Galla (2006) in the context of nonsymmetric ones. Importantly, the precise shape of the distribution from which the matrix entries are drawn does not matter; the mean and the variance fix all relevant properties of the matrix (Appendix B, Section B4). The matrix \mathbf{C} of intraspecific coefficients has zeros on the offdiagonal and each diagonal entry is sampled from some distribution with mean $\mu_d < 0$ and variance V_d . The full interaction matrix is then given by $\mathbf{A} = \mathbf{B} + \mathbf{C}$. In constructing the matrices, we keep all entries of \mathbf{A} nonpositive.

For random matrices, one can immediately obtain analytical stability criteria: for S large, the rightmost eigenvalue β_1 of \mathbf{B} depends not on any of the fine details of the interactions within the community, but only on the number of species S , the mean μ , and the variance V via

$$\beta_1 \approx 2\sqrt{SV} - \mu \quad (3)$$

(Appendix B, Section B4), where the approximation improves with increasing S . Combining with Weyl's inequalities (Eq. 2), we obtain $\gamma_S < \mu - 2\sqrt{SV}$ and $\gamma_1 < \mu - 2\sqrt{SV}$ as approximations to the necessary and sufficient conditions for stability, respectively in the case of large S . Of course, for small communities, the approximation of β_1 is less accurate and correspondingly the inequalities may not hold absolutely.

There are three implications of this result. First, note that a matrix \mathbf{A} can always be stabilized by making its diagonal entries larger in magnitude than the sum of the magnitudes of the other entries in the same row ("diagonal dominance"; the stability of such a matrix follows directly from Gershgorin's circle theorem). If the offdiagonal entries have an average value of μ , then for S large, one would expect γ_1 to have to scale with S to achieve stability. Instead, from Eq. (3) it is clear that γ_1 only needs to scale with \sqrt{S} , meaning that much weaker intraspecific coefficients are sufficient to stabilize coexistence. For instance, in a community of 100 species, γ_1 would need to be proportional to $\sim 10\mu$ instead of $\sim 100\mu$.

Second, β_1 scales with \sqrt{V} as well. The variance of the interspecific interaction strengths thus has a very important effect on stability: all other things being equal, communities with a smaller variance are easier to stabilize than communities with larger variances.

Third, μ must of course be a negative number in competitive systems, measuring the average competitive effect of one species on another across the community. It therefore impacts the amount of intraspecific stabilization required for coexistence via Eq. (3). However, for S large, the effect of μ in the expression $\gamma_1 < \mu - 2\sqrt{SV}$ is going to be dominated by the square root term. For large communities, we expect the mean interaction strength μ to be much less important in determining stability than the variance V .

This means that, for species-rich assemblages, intraspecific competition has to be not just stronger, but substantially stronger than average interspecific competition. Using the condition $\gamma_1 < \mu - 2\sqrt{SV}$, if the interspecific coefficients are uniformly sampled from $[-1, 0]$ ($\mu = -1/2$,

$V = 1/12$), then for $S = 12$ we get $\gamma_1 < -2.5 = 5\mu$, while $S = 300$ leads to $\gamma_1 < -10.5 = 21\mu$, with intraspecific effects having to be at least 21 times stronger than interspecific ones to achieve stability.

3.3 Nonrandom interspecific interaction matrices

What is the effect of a nonrandom community structure on competitive coexistence? We now take the original, randomly assembled matrix \mathbf{B} and rearrange its entries to obtain the minimum/maximum possible values for β_1 (Figure 1; note that, for β_1 minimal, species are sorted in increasing order of the leftmost eigenvector's entries, while for β_1 random and β_1 maximal, they are sorted in increasing order of the rightmost eigenvector's entries). Both the minimum and maximum β_1 cases possess a characteristic structure. The minimum β_1 case is perfectly hierarchical (Staniczenko et al. 2013): interaction strengths always decrease moving downwards and right when starting from the top left entry of the matrix. The maximum β_1 case is also hierarchical (here competitive effects always increase going upwards and right—or downwards and left—in the matrix, starting anywhere along the main diagonal), but in addition, one can also classify the species into two roughly distinct groups, with competitive interactions significantly weaker within than between those groups.

Both these scenarios have ecological interpretations. For the minimum β_1 case, consider a resource continuum. Now imagine that Species 1 consumes some range of these resources. Species 2 consumes a proper subset of the resources Species 1 consumes, Species 3 a proper subset of the resources Species 2 consumes, and so on, with the resource spectrum of Species S being the narrowest and a proper subset of the resource spectra of all the other species. Assume now that the competition coefficients are proportional to the overlap in resource use, and we end up with the structure in the top left of Figure 1. Since this arrangement leads to the smallest β_1 possible, this biological scenario is the easiest to stabilize from a dynamical perspective.

For the maximum β_1 case, imagine a unidimensional trait axis along which the intensity of competition is an *increasing* function of trait difference, instead of the usual assumption of decreasing competition. For instance, the axis could describe the quality of toxin produced by species of allelopathic plants, where each plant species is more resistant to toxins that are similar to its own. If we now assume that the species are sorted into two groups and that between-group distances along the axis are much larger than within-group distances, we get the structure in the bottom left of Figure 1. This scenario is also the most difficult to stabilize, since it produces the largest leading eigenvalue β_1 possible with the given set of coefficients.

One can look at the structure of interactions in a different, pairwise way (Figure 2). We line up all 50 species of the community horizontally, and connect two species by a blue arc if they would coexist in isolation (intraspecific competition greater than interspecific competition between them), and with a red arc if they would not. In the minimum β_1 case, red arcs disappear in a pattern from right to left as intraspecific competition is increased, reflecting species' positions in the hierarchy. In the maximum β_1 case, two clear groups emerge as intraspecific competition is increased: those within the groups can coexist pairwise, but those across the groups cannot, in line with the biological interpretation given above. The size of the groups is dictated by the relative strength of intra- to interspecific competition. In all cases, there can be no coexistence in the limit of no intraspecific competition, while in the case of strong intraspecific competition all species pairs would coexist in isolation—though, as discussed before, this does not guarantee community-wide coexistence.

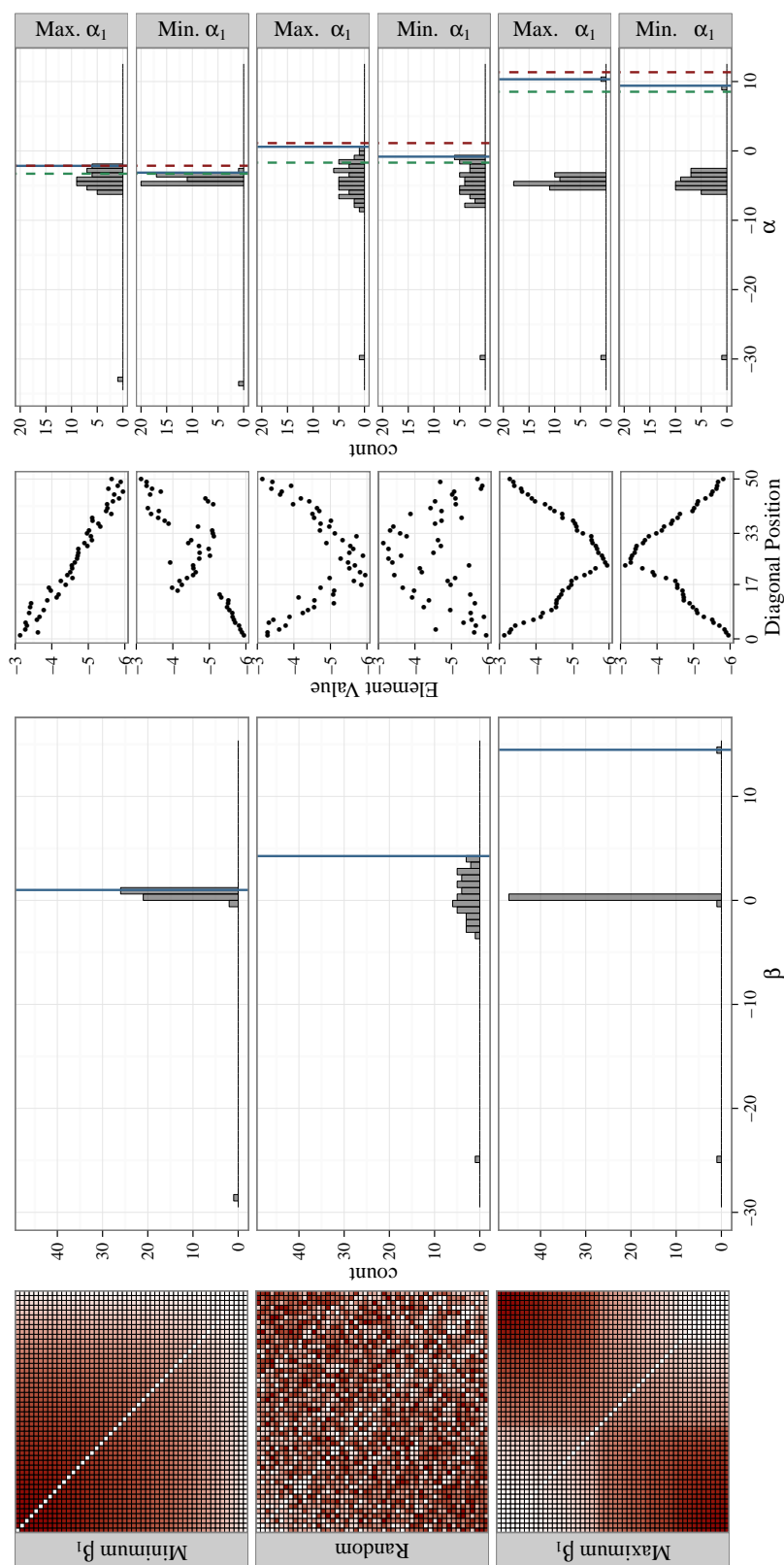


Figure 1: Columns from left to right: first, matrices of interspecific competition coefficients \mathbf{B} in a 50-species community with the same set of interaction strengths (uniformly sampled from $[-1, 0]$), but arranged in three different ways: minimizing the rightmost eigenvalue β_1 (top), random arrangement (middle), and maximizing β_1 (bottom). Darker colors correspond to stronger coefficients. While the minimizing case (top) is sorted in increasing order of the components of the eigenvector corresponding to the leftmost eigenvalue, the other two are sorted in increasing order of the components of the eigenvector associated with the rightmost eigenvalue. Second, histograms of the eigenvalue distributions of matrices depicted in the first column. The solid blue line marks the precise position of the rightmost eigenvalue β_1 . Third, for each matrix \mathbf{B} in column one, the coefficients of matrix \mathbf{C} (uniformly sampled from $[-6, -3]$) are rearranged to provide the maximum and minimum α_1 . The arrangement of these coefficients is plotted, sorted according to their position in the matrices in column one. Fourth, histograms of the eigenvalue distributions of $\mathbf{A} = \mathbf{B} + \mathbf{C}$, where \mathbf{B} is given in the first column, and \mathbf{C} is a matrix of intraspecific effects, with diagonal entries indicated by column three. The solid blue line again marks the precise position of the rightmost eigenvalue α_1 , and the dashed green/red lines are the bounds on the rightmost eigenvalue calculated from Eq. (2). (See the Supplementary Figures S1–S20 for replicates with different parameterizations, showing the robustness of the results.)

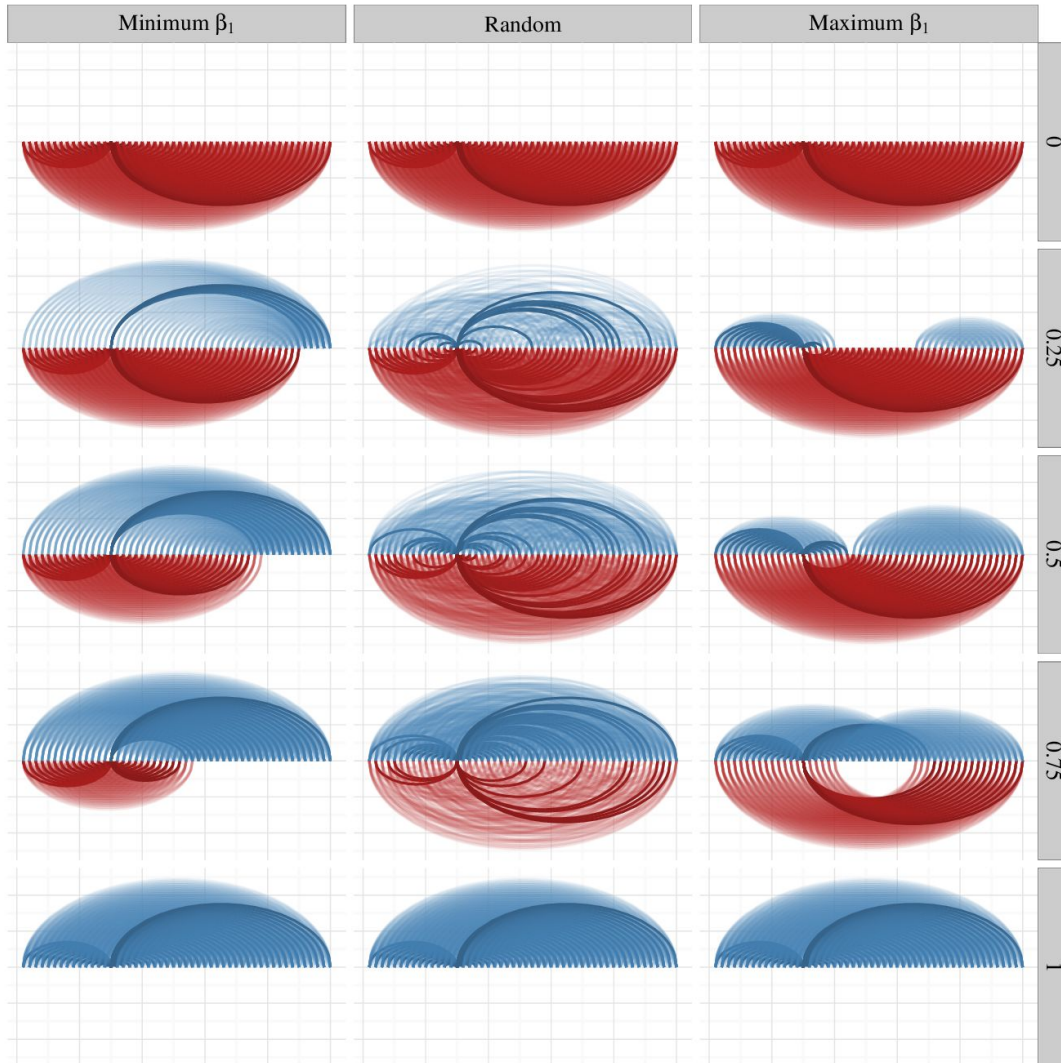


Figure 2: Pairwise interactions in a 50-species competitive community. Columns correspond to different arrangements of the interspecific interaction matrix \mathbf{B} : minimizing its rightmost eigenvalue β_1 (left), random (middle), and maximizing β_1 (right). Rows correspond to different values of the intraspecific competition coefficient, here assumed to be the same for all species. In each panel, a blue/red connection between two species means that those two species could/could not coexist in a pairwise manner. Highlighted arcs are interactions of a particular species (arbitrarily chosen to be the 15th species from the left in each ordering). Note the regular patterns of blue and red arcs emerging in the minimum and maximum β_1 columns, reflecting the community structures seen on Figure 1.

4 Intraspecific competition and community stability

Once we arrange the matrix \mathbf{B} of interspecific coefficients to minimize/maximize β_1 , we can ask how one should distribute a given set of intraspecific coefficients \mathbf{C} across species to obtain the smallest/largest value of α_1 , the rightmost eigenvalue of the full interaction matrix \mathbf{A} determining overall community stability.

Figure 1 shows how the eigenvalue distribution changes according to the arrangement of intra- and interspecific coefficients. For each arrangement of interspecific competition coefficients, we found the arrangement of intraspecific ones minimizing and maximizing the rightmost eigenvalue α_1 of \mathbf{A} . While each of the six cases exhibits a different pattern, they are all consistent with a simple rule of thumb: to maximize α_1 , stronger intraspecific entries should be associated with species whose interspecific interaction strengths have smaller variance, and vice versa. Conversely, to minimize α_1 , stronger intraspecific coefficients should be paired with larger variance in interspecific interaction strengths. For example, to maximize α_1 in the minimum β_1 case in Figure 1, the first species should be assigned the weakest intraspecific interaction, the second species the second weakest, and so on, with the S th species (smallest variance in interspecific interaction strengths) having the strongest one.

These patterns are only approximate, and are noticeably fuzzy in the case where both β_1 and α_1 are minimized, and in both of the random cases¹. We do not know whether our rule of thumb is indeed a general rule. However, It can be shown that the observed patterns are always the theoretically expected ones in our particular scenarios (Appendix B, Section B6). A more intuitive explanation can also be given. In general, a higher variance in the interspecific effects also implies a larger absolute magnitude of the strongest intraspecific effect experienced by a species (Figure 1). Assigning the weakest interspecific coefficients to species with the highest variance is therefore the most likely way of violating Sylvester's necessary criterion that all species pairs follow the two-species rule for coexistence, destabilizing the system.

5 Feasibility

Dynamical instability precludes, but dynamical stability does not guarantee coexistence: the equilibrium solution also needs to be feasible, i.e., $\mathbf{n} = -\mathbf{A}^{-1}\mathbf{b}$ needs to be strictly positive. For two species, writing $\mathbf{b} = (\cos \theta, \sin \theta)$ where θ defines the direction of \mathbf{b} , this translates into the the feasibility condition

$$\arctan\left(\frac{A_{21}}{A_{11}}\right) < \theta < \arctan\left(\frac{A_{22}}{A_{12}}\right) \quad (4)$$

(Appendix B, Section B2.2). That is, for any given interaction matrix \mathbf{A} , one can determine all directions of \mathbf{b} leading to a feasible equilibrium. This is best expressed via the concept of the *feasibility domain* Ξ , the proportion of feasible directions to all possible directions (Svirezhev and

¹One might wonder why there is a pattern to the random cases at all. The answer is that species are ordered by the leading eigenvector, which is nonrandom with respect to the (otherwise randomly determined) variance of the rows' entries. See the random case in Figure 1: there is a visible trend for stronger coefficients towards the upper right and lower left corners of the matrix.

Logofet 1983, Rohr et al. 2014, Grilli et al. 2015). In the two-species case,

$$\Xi = \frac{2}{\pi} \max \left\{ \arctan \left(\frac{A_{22}}{A_{12}} \right) - \arctan \left(\frac{A_{21}}{A_{11}} \right), 0 \right\}. \quad (5)$$

Below, instead of Ξ , we use the (geometric) average feasible domain *per dimension* $\sqrt[n]{\Xi}$, a more meaningful metric which makes feasibility comparable across systems with different numbers of species (Appendix B, Section B7).

To explore the effect of intra- and interspecific interaction strengths on the feasibility of competitive communities, we obtained $\sqrt[n]{\Xi}$ via numerical integration (Appendix B, Section B7) for all three cases of distributing the interspecific interaction strengths: minimum β_1 , random, and maximum β_1 . For each of the three cases we gradually increased the strength of overall intraspecific competition, assumed to be the same for all species. We only calculated the feasibility domain for stable matrices, since a feasible unstable equilibrium does not describe coexistence. We know a priori that $\sqrt[n]{\Xi}$ must be zero at the boundary of stability and instability where the rightmost eigenvalue crosses the origin of the complex plane, because at this point the model is structurally unstable. As intraspecific competition is increased from this point on, the matrices invariably obtain larger domains of feasibility $\sqrt[n]{\Xi}$ (Figure 3). Surprisingly, after an initial, very steep increase of feasibility from zero up, $\sqrt[n]{\Xi}$ settles down to the same characteristic curve independent of the structure of interspecific interactions. In the big picture, intraspecific competition has the most influence on feasibility, whereas interspecific competition has the role of determining the point at which the community becomes stable in the first place.

6 Discussion

In this work we explored the relationship between intra- and interspecific competition and its effect on coexistence in multispecies competitive communities. Our strategy was to decompose the interaction matrix into intra- and interspecific parts, allowing us to bound the stability of the community in terms of their eigenvalues via Weyl's inequality. We could then obtain simple stability criteria for random competitive communities. Using the random case as a springboard, we searched for the community structures that minimize/maximize the rightmost eigenvalue of the interaction matrix, both in terms of intra- and interspecific effects. Both the most and the least stabilized case exhibited a characteristic interspecific structure, with a hierarchical arrangement of coefficients, and a quasi-bipartite structure in the least stabilized configuration. Intraspecific effects were most stabilizing when species with the largest variance in interspecific interactions were assigned strong intraspecific coefficients, and most destabilizing when they were assigned weak ones. The feasible fraction of parameter space invariably increased with a decreasing rightmost eigenvalue, showing that systems that are more likely to be stable are also more robust against environmental perturbations of the intrinsic growth rates.

Conclusions about the relationship between intra- and interspecific competition have largely stemmed from experiments and analyses which considered very few (usually two) species (e.g., Chase et al. 2002, Bolker et al. 2003, Abrams and Wilson 2004, Forrester et al. 2006, Adler et al. 2007, Murrell 2010, Hasegawa et al. 2014). In this case, the conditions for the stability of the interaction matrix translate into simple inequalities containing the competition coefficients, with the direct biological interpretation that species must limit themselves more than their competitors for

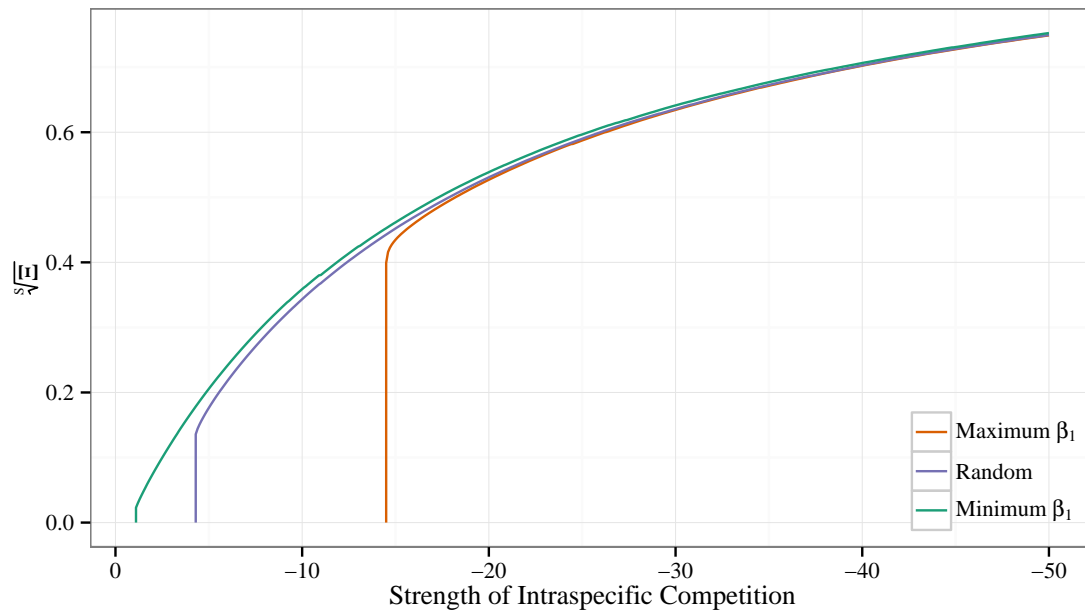


Figure 3: The feasibility domain $\sqrt[S]{\Xi}$ as a function of intraspecific interaction strength, assumed here to be constant across $S = 50$ species. The curves correspond to β_1 maximized (orange), β_1 corresponding to a random competition matrix (purple), and β_1 minimized (green), where β_1 is the rightmost eigenvalue of the matrix \mathbf{B} of interspecific competition coefficients. Note that the abscissa is reversed in order to better indicate increasing strength of intraspecific competition. In each case, $\sqrt[S]{\Xi}$ is plotted only for stable matrices. Except for the discrepancy near the boundary between stability and instability, all three cases eventually converge on the same characteristic feasibility curve for any strength of intraspecific competition.

coexistence. As the number of species increases, the Routh-Hurwitz stability criteria (Edelstein-Keshet 1988) grow in number and complexity; each must be satisfied for stability, yet their biological implications are no longer easily derived. Therefore, in general, there is no simpler way to answer the question of stability than to state that “the rightmost eigenvalue has to be in the left half plane”. The necessary condition for symmetric matrices that all species pairs must individually satisfy the familiar two-species coexistence condition is a convenient exception to this rule.

Two-species competitive communities have a simple and transparent structure. For multiple species, many different structures are possible, with large effects on community stability. We have shown that the same set of coefficients can lead to vastly different stability properties: communities that were most stabilized (hierarchical arrangement) or least stabilized (hierarchy, but with two groups and weak interactions within, strong interaction between group members) both exhibited a characteristic structure. The wide range of possible rightmost eigenvalues for the exact same set of coefficients, with only the community structure varying, is one of the main reasons why there is no trivial generalization of the two-species coexistence rule to multispecies communities. Nevertheless, it is often implied, without being explicitly stated, that the two-species criterion holds for an arbitrary number of species (Barot 2004, Amarasekare et al. 2004, Chesson et al. 2004, Adler

et al. 2007, Chesson 2011, Houseman 2014). It does not—except as a necessary but insufficient stability condition for symmetric interaction matrices only.

Of course, it must be true in a broader sense that, in order to coexist, species must limit themselves more strongly than they limit their competitors: if we add individuals to a species at a stable attractor, that same number of individuals will eventually die and the community will return to its state prior to the perturbation. Attributing this return exclusively to the relative strength of intra- and interspecific competition between pairs of species, however, potentially ignores the myriad indirect higher-order feedbacks influencing species trajectories, which can override the simple two-species coexistence rule. For instance, in reactive systems a perturbation to species abundances may initially be amplified before returning to equilibrium (Neubert and Caswell 1997, Tang and Allesina 2014). In such cases, the overall requirement for stability does not translate directly into a straightforward rule for the competition coefficients themselves. Interestingly, symmetric matrices cannot be reactive—the same situation for which there *is* a reasonably straightforward generalization of the two-species rule of coexistence.

What can be said about nonsymmetric interaction matrices? Even in cases where symmetric competition is a consequence rather than an assumption of the model in question (MacArthur 1972, Roughgarden 1979, Case 2000, Hernández-García et al. 2009), other confounding factors not included in the model will likely distort perfect symmetry. In other cases, such as size-structured competition for light in forest trees (Kohyama 1993, 2006, Adams et al. 2007), asymmetry is an essential part of the system's ecology.

We do not expect our results to change substantially for mild degrees of asymmetry, since that can be accounted for as a small perturbation to the symmetric model. For substantial asymmetry however, several difficulties emerge, rendering most of the techniques applied in this work inapplicable (see Appendix A). Some conclusion can still be made though for random competitive communities, as long as the variance of the intraspecific effects around a mean γ is not very large. Then one can derive the stability condition $\gamma > (1 + \rho)\sqrt{SV} - \mu$, with ρ being the average correlation between the effect of species i on j and the effect of j on i . For strongly negative values of ρ , this implies that interspecific effects can be much larger than intraspecific ones and coexistence can still be stable, at least locally. In fact, the aforementioned case of size-structured competition for light in forests, where taller trees have a much larger effect on shorter ones than vice versa, presents an example where negative values of ρ are expected. Such systems could then be stabilized by much weaker intraspecific effects than corresponding symmetric cases. It is interesting to wonder whether and how much this structural property is responsible for explaining the general prevalence of such hierarchical competitive systems. Whether their stability is in fact explained in this way awaits further investigations.

Acknowledgements

We thank R. D'Andrea, J. Grilli, G. Kylafis, A. Ostling, L. Pásztor, R. Rael, and E. Sander for discussions. Comments by M. Leibold, D. Stouffer, and an anonymous reviewer all helped improve the clarity of the manuscript. This work was supported by NSF #1148867.

References

- Abrams, P. A., and W. G. Wilson. 2004. Coexistence of competitors in metacommunities due to spatial variation in resource growth rates; does R^* predict the outcome of competition? *American Naturalist* 7:929–940.
- Adams, T. P., D. W. Purves, and S. W. Pacala. 2007. Understanding height-structured competition in forests: is there an R^* for light? *Proceedings of the Royal Society B* 274:3039–3047.
- Adler, P. B., S. P. Ellner, and J. M. Levine. 2010. Coexistence of perennial plants: an embarrassment of niches. *Ecology Letters* 13:1019–1029.
- Adler, P. B., J. Hillerislambers, and J. M. Levine. 2007. A niche for neutrality. *Ecology Letters* 10:95–104.
- Amarasekare, P., M. F. Hoopes, N. Mouquet, and M. Holyoak. 2004. Mechanisms of coexistence in competitive metacommunities. *American Naturalist* 164:310–326.
- Barabás, G., S. Pigolotti, M. Gyllenberg, U. Dieckmann, and G. Meszéna. 2012. Continuous coexistence or discrete species? A new review of an old question. *Evolutionary Ecology Research* 14:523–554.
- Barot, S. 2004. Mechanisms promoting plant coexistence: can all the proposed processes be reconciled? *Oikos* 106:185–192.
- Bolker, B. M., S. W. Pacala, and C. Neuhauser. 2003. Spatial Dynamics in Model Plant Communities: What Do We Really Know? *American Naturalist* 162:135–148.
- Case, T. J. 1990. Invasion resistance arises in strongly interacting species-rich model competition communities. *Proceedings of the National Academy of Sciences USA* 87:9610–9614.
- . 2000. *An Illustrated Guide to Theoretical Ecology*. Oxford University Press, New York.
- Chase, J. M., P. A. Abrams, J. P. Grover, S. Diehl, P. Chesson, R. D. Holt, S. A. Richards, R. M. Nisbet, and T. J. Case. 2002. The interaction between predation and competition: a review and synthesis. *Ecology Letters* 5:302–315.
- Chesson, P. 1994. Multispecies competition in variable environments. *Theoretical Population Biology* 45:227–276.
- . 2000. Mechanisms of maintenance of species diversity. *Annual Review of Ecology and Systematics* 31:343–366.
- . 2009. Scale transition theory with special reference to species coexistence in a variable environment. *Journal of Biological Dynamics* 3:149–163.
- . 2011. Ecological niches and diversity maintenance. Pages 43–60 *in* *Research in Biodiversity-Models and Applications*. InTech, Rijeka, Croatia.
- Chesson, P., and S. Ellner. 1989. Invasibility and stochastic boundedness in two-dimensional competition models. *Journal of Mathematical Biology* 27:117–138.

- Chesson, P., R. L. E. Gebauer, S. Schwinning, N. Huntly, K. Wiegand, M. S. K. Ernest, A. Sher, A. Novoplanski, and J. F. Weltzin. 2004. Resource pulses, species interactions, and diversity maintenance in arid and semi-arid environments. *Oecologia* 141:236–253.
- Diederich, S., and M. Oppen. 1989. Replications with random interactions: a solvable model. *Physical Review A* 39:4333–4336.
- Edelstein-Keshet, L. 1988. *Mathematical models in biology*. Random House, New York, USA.
- Edwards, K. F., and S. J. Schreiber. 2010. Preemption of space can lead to intransitive coexistence of competitors. *Oikos* 119:1201–1209.
- Forrester, G. E., B. Evans, M. A. Steele, and R. R. Vance. 2006. Assessing the magnitude of intra- and interspecific competition in two coral reef fishes. *Oecologia* 148:632–640.
- Fulton, W. 2000. Eigenvalues, invariant factors, highest weights, and Schubert calculus. *Bulletin of the American Mathematical Society* 37:209–249.
- Galla, T. 2006. Random replicators with asymmetric couplings pages arXiv:cond-mat/0508174v3 [cond-mat.dis-nn].
- Gotelli, N. J. 2008. *A primer of ecology*. Sinauer Associates, Sunderland, Massachusetts, USA.
- Grilli, J., M. Adorisio, S. Suweis, G. Barabás, J. R. Banavar, S. Allesina, and A. Maritan. 2015. The geometry of coexistence in large ecosystems pages arXiv:1507.05337 [q-bio.PE].
- Hasegawa, K., K. Morita, K. Ohkuma, T. Ohnuki, and Y. Okamoto. 2014. Effects of hatchery chum salmon fry on density-dependent intra- and interspecific competition between wild chum and masu salmon fry. *Canadian Journal of Fisheries and Aquatic Sciences* 71:1475–1482.
- Hernández-García, E., C. López, S. Pigolotti, and K. H. Andersen. 2009. Species competition: coexistence, exclusion and clustering. *Philosophical Transactions of the Royal Society London, Series A* 367:3183–3195.
- Houseman, G. R. 2014. Aggregated seed arrival alters plant diversity in grassland communities. *Journal of Plant Ecology* 7:51–58.
- Justus, J. 2006. Loop analysis and qualitative modeling: limitations and merits. *Biology and Philosophy* 21:647–666.
- Kohyama, T. 1993. Size-structured tree populations in gap-dynamic forest—the forest architecture hypothesis for the stable coexistence of species. *Journal of Ecology* 81:131–143.
- . 2006. The effect of patch demography on the community structure of forest trees. *Ecological Research* 21:346–355.
- Law, R., and R. D. Morton. 1996. Permanence and the assembly of ecological communities. *Ecology* 77:762–775.
- Leibold, M. A., and M. A. McPeck. 2006. Coexistence of the niche and neutral perspectives in community ecology. *Ecology* 87:1399–1410.

- Levine, J. M., and J. HilleRisLambers. 2009. The importance of niches for the maintenance of species diversity. *Nature* 461:254–258.
- Levine, J. M., and M. Rees. 2004. Effects of temporal variability on rare plant persistence in annual systems. *American Naturalist* 164:350–363.
- Levins, R. 1968. *Evolution in changing environments*. Princeton University Press, Princeton.
- . 1974. Qualitative analysis of partially specified systems. *Ann. NY Acad. Sci.* 231:123–138.
- . 1975. Evolution in communities near equilibrium. Pages 16–50 *in* M. Cody and J. M. Diamond, eds. *Ecology and Evolution of Communities*. Harvard University Press, Cambridge.
- MacArthur, R. H. 1972. *Geographical ecology*. Harper & Row, New York.
- MacArthur, R. H., and R. Levins. 1967. Limiting similarity, convergence, and divergence of coexisting species. *American Naturalist* 101:377–385.
- May, R. M. 1973. *Stability and Complexity in Model Ecosystems*. Princeton University Press, Princeton.
- May, R. M., and W. J. Leonard. 1975. Nonlinear aspects of competition between three species. *SIAM Journal on Applied Mathematics* 29:243–253.
- Meszéna, G., M. Gyllenberg, L. Pásztor, and J. A. J. Metz. 2006. Competitive exclusion and limiting similarity: a unified theory. *Theoretical Population Biology* 69:68–87.
- Mittelbach, G. G. 2012. *Community Ecology*. Sinauer Associates, Sunderland, Massachusetts, USA.
- Murrell, D. J. 2010. When does local spatial structure hinder competitive coexistence and reverse competitive hierarchies? *Ecology* 91:1605–1616.
- Neubert, M. G., and H. Caswell. 1997. Alternatives to resilience for measuring the responses of ecological systems to perturbations. *Ecology* 78:653–665.
- Opper, M., and S. Diederich. 1992. Phase transition and $1/f$ noise in a game dynamical model. *Physical Review Letters* 69:1616–1619.
- O’Rourke, S., and D. Renfrew. 2014. Low rank perturbations of large elliptic random matrices. *Electronic Journal of Probability* 19:1–65.
- Rohr, R. P., S. Saavedra, and J. Bascompte. 2014. On the structural stability of mutualistic systems. *Science* 345.
- Roughgarden, J. 1979. *Theory of Population Genetics and Evolutionary Ecology: an Introduction*. Macmillan, New York.
- Siepielski, A. M., K. L. Hung, E. E. B. Bein, and M. A. McPeck. 2010. Experimental evidence for neutral community dynamics governing an insect assemblage. *Ecology* 91:847–857.

- Siepielski, A. M., and M. A. McPeck. 2010. On the evidence for species coexistence: a critique of the coexistence program. *Ecology* 91:3153–3164.
- Sommers, H. J., A. Crisanti, H. Sompolinsky, and Y. Stein. 1998. Spectrum of large random asymmetric matrices. *Physical Review Letters* 60:1895–1898.
- Staniczenko, P. P. A., J. C. Kopp, and S. Allesina. 2013. The ghost of nestedness in ecological networks. *Nature Communications* 4:1391.
- Svirezhev, Y. M., and D. O. Logofet. 1983. *Stability of Biological Communities*. Mir Publishers, Moscow, Russia.
- Tang, S., and S. Allesina. 2014. Reactivity and stability of large ecosystems. *Frontiers in Ecology and Evolution*.
- Vandermeer, J. H., and D. E. Goldberg. 2013. *Population ecology: First principles*. 2nd edition. Princeton University Press, Princeton, New Jersey.

Appendix A: The case of nonsymmetric interaction matrices

When the interaction matrix \mathbf{A} is nonsymmetric, substantial complications emerge which make it difficult to say much about the relationship between intra- and interspecific competition and coexistence. First, Sylvester's criterion no longer applies, therefore there is no guarantee that a species pair violating the two-species coexistence rule will lead to the loss of coexistence (see Appendix B, Section B2.3 for a three-species, and Figure A1 for a 50-species example). Second, local stability no longer guarantees global stability of coexistence, and local instability does not mean the lack of coexistence, e.g., along some periodic or chaotic orbit (Appendix B, Section B2.3 and Section B2.4). Third, \mathbf{A} no longer determines stability; instead, the Jacobian evaluated at the equilibrium $\mathbf{n} = -\mathbf{A}^{-1}\mathbf{b}$ does. This reads $\mathbf{J} = \text{diag}(\mathbf{n})\mathbf{A} = -\text{diag}(\mathbf{A}^{-1}\mathbf{b})\mathbf{A}$ (Appendix B, Section B2.1). Since \mathbf{J} now depends on the intrinsic rates, it is impossible to give a formal coexistence criterion independent of \mathbf{b} . Fourth, Weyl's inequality no longer holds, making the decomposition of \mathbf{J} into intra- and interspecific parts ineffective.

Despite these difficulties, some conclusions can still be made for random asymmetric competitive communities. As long as the variance of the equilibrium densities is small, we have $\text{diag}(\mathbf{n}) \approx \bar{n}\mathbf{I}$, where \bar{n} is the average abundance and \mathbf{I} is the identity matrix. Then, $\mathbf{J} = \text{diag}(\mathbf{n})\mathbf{A} \approx \bar{n}\mathbf{A}$, therefore \mathbf{A} still determines stability, albeit only locally. If we now perform the $\mathbf{A} = \mathbf{B} + \mathbf{C}$ decomposition where \mathbf{B} contains the interspecific and \mathbf{C} the intraspecific coefficients, one can apply the elliptic law of random matrix theory (Sommers et al. 1998, O'Rourke and Renfrew 2014; Appendix B, Section B4.2) to find the leading eigenvalue β_1 of \mathbf{B} :

$$\beta_1 \approx (1 + \rho)\sqrt{SV} - \mu, \quad (\text{A1})$$

where ρ is the average correlation between B_{ij} and B_{ji} . Then, as long as the variance of the intraspecific effects around a mean γ is not too large (i.e., $\mathbf{C} \approx \gamma\mathbf{I}$), we have the stability condition

$$\gamma > (1 + \rho)\sqrt{SV} - \mu \quad (\text{A2})$$

(Appendix B, Section B4).

Due to the similarity of Eqs. (3) and (A1), much same conclusions apply as in the symmetric case—but only as long as ρ is positive or not too strongly negative. Strong negative correlations on the other hand can substantially reduce the amount of intraspecific competition required for stability. As an extreme example, if $\rho = -1$, then $\beta_1 = -\mu$, and therefore $\gamma < \mu$ will lead to stability regardless of the number of species S or the variance V in interspecific effects. Even if the variance is much larger than the mean, stability is ensured. In other words, for strongly negative values of ρ , interspecific competitive effects may dominate over intraspecific ones, and the system can still be stable. See Figure A1 for an example with $\gamma = -2.2$, $\mu = -2$, $V = 0.3$, and $\rho = -0.95$.

The most important restrictive assumption above is that the variance of the species abundances around \bar{n} is small. Real communities, on the other hand, possess a characteristic species abundance distribution close to lognormal, with a large variance (McGill et al. 2007). Moreover, theoretical investigations of the species abundance distribution under the replicator dynamics with both symmetric (Tokita 2004) and nonsymmetric (Yoshino et al. 2008) payoff matrices have arrived at the exact same conclusion. The species abundance distributions produced by the model are therefore consistent with empirically observed ones, rendering the assumption of nearly equal equilibrium abundances implausible.

However, preliminary explorations (Allesina and Tang 2015) show that when the equilibrium abundances \mathbf{n} follow realistic species abundance distributions, the elliptic law consistently overestimates the leading eigenvalue. That is, $\bar{n}\mathbf{A}$ always has a larger leading eigenvalue than $\text{diag}(\mathbf{n})\mathbf{A}$, and sometimes substantially so. Eq. (A1) can therefore be seen as a conservative estimate of stability. We therefore expect this criterion, based on the elliptic law, to provide a sufficient stability condition for realistic communities.

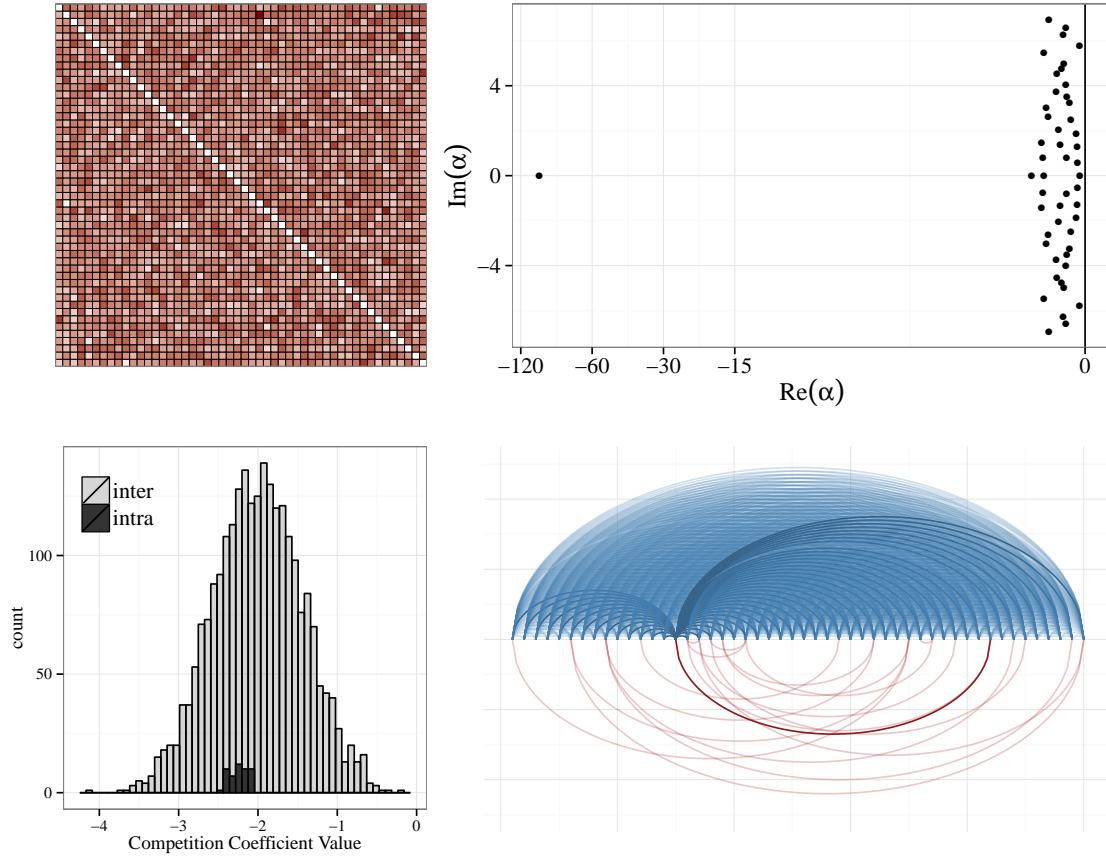


Figure A1: A highly asymmetric, stable competitive community of 50 species. Interspecific coefficient pairs (B_{ij}, B_{ji}) were randomly drawn from a bivariate normal distribution with marginal means $\mu = -2$, marginal variances $V = 0.3$, and correlation $\rho = -0.95$. Intraspecific coefficients C_{ii} were uniformly sampled from $[-2.4, -2]$. Top left: the matrix \mathbf{B} of interspecific coefficients. Top right: eigenvalue distribution of $\mathbf{A} = \mathbf{B} + \mathbf{C}$ in the complex plane. Since all eigenvalues have negative real parts, the system is locally stable. Bottom left: distribution of intra- and interspecific interaction strengths; note the substantially larger variance of the interspecific coefficients. Bottom right: species (nodes) connected by blue/red arcs if they can/cannot coexist as pairs. Highlighted arcs are connections of species no. 15. Note that several species pairs violate the pairwise coexistence rule, yet the community as a whole is locally stable.

Appendix B: Supporting Information

B1 Dynamical stability, structural stability, and feasibility

Consider an autonomous dynamical system with S variables n_1, \dots, n_S (representing species abundances or biomasses) and parameters μ_1, \dots, μ_k :

$$\frac{dn_i}{dt} = f_i(n_1, \dots, n_S, \mu_1, \dots, \mu_k), \quad (\text{B1})$$

where t is time, and the f_i are functions of the n_i and the model parameters (the time-dependence of the n_i is suppressed for notational convenience). An equilibrium of the system is a set of values $\hat{n}_1, \dots, \hat{n}_S$ such that all rates of change are simultaneously zero:

$$f_i(\hat{n}_1, \dots, \hat{n}_S, \mu_1, \dots, \mu_k) = 0 \quad (\text{B2})$$

for all $i = 1, \dots, S$. The *local dynamical stability* of an equilibrium can be determined by inspecting the eigenvalues of the Jacobian matrix $J_{ij} = \partial f_i / \partial n_j$ evaluated at the equilibrium: stability requires that all eigenvalues have negative real parts. An equilibrium that is not locally dynamically stable is called (locally, dynamically) unstable. A “stable matrix” is one with all its eigenvalues having negative real parts.

The dynamics is said to be *structurally stable* if sufficiently small perturbations of the parameters μ_1, \dots, μ_k cannot qualitatively alter the behavior of the system’s trajectories. Equilibria with eigenvalues sitting exactly on the imaginary axis present an example of structural instability, as an arbitrarily small perturbation could in principle tip those eigenvalues either in the stable or the unstable direction in the complex plane, qualitatively changing system behavior.

The values of the abundances n_i at an equilibrium point are in principle arbitrary. However, in ecological systems we are usually interested in equilibria that are strictly positive, i.e., $n_i > 0$ for all i . These are called *feasible* equilibrium points.

B2 The Lotka–Volterra model

B2.1 General properties

The generalized Lotka–Volterra model for S species with abundances n_1, \dots, n_S can be written

$$\frac{dn_i}{dt} = n_i \left(b_i + \sum_{j=1}^S A_{ij} n_j \right), \quad (\text{B3})$$

where b_i is the intrinsic growth rate of species i , and the A_{ij} are interaction coefficients: A_{ij} measures the amount of change in species i ’s per capita growth rate caused by a unit change in species j ’s density.

The equation can be written in vector form. Collecting the coefficients b_i into the vector \mathbf{b} , the abundances n_i into the vector \mathbf{n} , the interaction coefficients A_{ij} into the matrix \mathbf{A} , and letting $\text{diag}(\mathbf{n})$ be the diagonal matrix with the entries of the vector \mathbf{n} along its diagonal and zeros elsewhere, Eq. (B3) reads

$$\frac{d\mathbf{n}}{dt} = \text{diag}(\mathbf{n})(\mathbf{b} + \mathbf{A}\mathbf{n}). \quad (\text{B4})$$

The Lotka–Volterra model with S species may have up to 2^S equilibria, out of which at most one is feasible. We call this the *coexistence equilibrium* (even when it does not describe actual coexistence). From Eq. (B4), this equilibrium is given when all the \mathbf{n} are assumed nonzero:

$$\mathbf{b} + \mathbf{A}\hat{\mathbf{n}} = 0, \quad (\text{B5})$$

where the hat denotes equilibrium values. Therefore,

$$\hat{\mathbf{n}} = -\mathbf{A}^{-1}\mathbf{b}, \quad (\text{B6})$$

with \mathbf{A}^{-1} being the inverse of \mathbf{A} . This equilibrium is feasible if $\hat{\mathbf{n}}$ is strictly positive. Note that if a vector \mathbf{b} leads to a feasible solution, so does the vector $\eta\mathbf{b}$ for an arbitrary positive constant η . Indeed, for $\mathbf{b}^* = \eta\mathbf{b}$ we get the solution $\hat{\mathbf{n}}^* = -\mathbf{A}^{-1}\mathbf{b}^* = -\mathbf{A}^{-1}\eta\mathbf{b} = \eta\hat{\mathbf{n}}$, which is still feasible if $\eta > 0$. For a given matrix \mathbf{A} therefore, only the direction of \mathbf{b} matters for feasibility, not its absolute magnitude. This opens the way for describing feasibility via the fraction of directions in which \mathbf{b} is feasible, out of all possible directions.

To determine the stability of the equilibrium given by Eq. (B6), we calculate the Jacobian \mathbf{J} with entries $J_{ij} = \partial(dn_i/dt)/\partial n_j$, using Eq. (B4). The result is $\mathbf{J} = \text{diag}(\mathbf{b} + \mathbf{A}\mathbf{n}) + \text{diag}(\mathbf{n})\mathbf{A}$. Evaluating \mathbf{J} at equilibrium, the first term cancels because $\hat{\mathbf{n}} = -\mathbf{A}^{-1}\mathbf{b}$, therefore we get $\mathbf{J}|_{\hat{\mathbf{n}}} = \text{diag}(\hat{\mathbf{n}})\mathbf{A} = -\text{diag}(\mathbf{A}^{-1}\mathbf{b})\mathbf{A}$. Stability of this matrix guarantees the local stability of the coexistence fixed point, though not its feasibility.

Important results follow if \mathbf{A} is a symmetric matrix with all negative entries; i.e., when interactions are purely competitive. We then have the following (MacArthur 1970, Hofbauer and Sigmund 1988, Hernández-García et al. 2009). First, the system cannot exhibit cycles, chaos, or any other behavior than simple convergence to a fixed point. Second, if $\hat{\mathbf{n}}$ is feasible and locally stable, it is globally stable as well. Third, stability of the coexistence equilibrium depends only on the stability of \mathbf{A} instead of the full Jacobian evaluated at equilibrium, $\mathbf{J}|_{\hat{\mathbf{n}}} = \text{diag}(\hat{\mathbf{n}})\mathbf{A}$. Since \mathbf{A} is symmetric, all its eigenvalues are real; as long as all of them are negative, the coexistence equilibrium is (globally) stable.

B2.2 Two species

In the well-known textbook example of the competitive two-species Lotka–Volterra equations, one has the great simplification that the coexistence equilibrium is globally stable or unstable even if \mathbf{A} is not symmetric (the easiest way to prove this is by constructing appropriate Lyapunov functions; see, e.g., Zeeman 1993). Therefore, if coexistence is locally stable, it is also globally stable. Based on this, four outcomes are possible:

1. No feasible equilibrium point exists; species 1 wins from any positive initial condition.
2. No feasible equilibrium point exists; species 2 wins from any positive initial condition.
3. There is a feasible equilibrium point but it is unstable; species 1 or 2 wins depending on initial conditions.
4. There is a feasible equilibrium point and it is stable; the two species coexist from any positive initial condition.

It should be mentioned that there are other, degenerate outcomes as well (for instance, the two species could be exactly identical in all their parameters, leading to a one-dimensional, neutrally stable manifold), but these examples are structurally unstable.

The coexistence equilibrium will be feasible if it is strictly positive: $\hat{\mathbf{n}} > \mathbf{0}$. Using Eq. (B6), this requirement can be written as $-\mathbf{A}^{-1}\mathbf{b} > \mathbf{0}$. Writing this inequality out in components for two species and simplifying, one arrives at

$$\frac{A_{12}}{A_{22}} < \frac{b_1}{b_2} < \frac{A_{11}}{A_{21}} \quad (\text{B7})$$

(e.g., Vandermeer 1975, Mallet 2012). This same set of conditions may be written in a slightly different form. As discussed before, only the direction of \mathbf{b} matters for feasibility, not its magnitude. We therefore parameterize the intrinsic growth rates as $\mathbf{b} = (\cos \theta, \sin \theta)$, i.e., \mathbf{b} has length 1, and $0 < \theta < \pi/2$ is the angle measured counterclockwise from the abscissa of the two-dimensional plane of possible \mathbf{b} vectors. Substituting this into Eq. (B7) and simplifying, we get

$$\arctan\left(\frac{A_{21}}{A_{11}}\right) < \theta < \arctan\left(\frac{A_{22}}{A_{12}}\right). \quad (\text{B8})$$

Expressing this as the proportion of feasible θ values out of all possible values $0 < \theta < \pi/2$, and calling this fraction Ξ , we get

$$\Xi = \frac{2}{\pi} \max\left\{\arctan\left(\frac{A_{22}}{A_{12}}\right) - \arctan\left(\frac{A_{21}}{A_{11}}\right), 0\right\}, \quad (\text{B9})$$

where $\max(\cdot, \cdot)$ picks the larger of the two arguments.

For dynamical stability, all eigenvalues of $\mathbf{J}|_{\hat{\mathbf{n}}} = \text{diag}(\hat{\mathbf{n}})\mathbf{A}$ (the Jacobian evaluated at the equilibrium point) must have negative real parts. For two species, and two species only, there is a shortcut: the coexistence equilibrium for competitive dynamics is stable if and only if \mathbf{A} has a positive determinant (Zeeman 1993). Writing this condition out, we get

$$\det(\mathbf{A}) = A_{11}A_{22} - A_{12}A_{21} > 0, \quad (\text{B10})$$

or, equivalently,

$$\sqrt{A_{11}A_{22}} > \sqrt{A_{12}A_{21}}. \quad (\text{B11})$$

The left hand side is the geometric mean of the two intraspecific competition coefficients, while the right hand side is the geometric mean of the interspecific coefficients.

This condition is often interpreted as intraspecific competition having to be stronger than interspecific competition for coexistence. Note that this is a necessary but not a sufficient coexistence condition, as Eq. (B7) also needs to be satisfied. While true in the form just presented, one should be careful not to overinterpret this simple result. For instance, consider the following parameterization of the two-species Lotka–Volterra model:

$$\mathbf{b} = \begin{pmatrix} 6 \\ 10 \end{pmatrix}, \quad \mathbf{A} = -\begin{pmatrix} 9 & 1 \\ 13 & 2 \end{pmatrix}. \quad (\text{B12})$$

This parameterization satisfies Eqs. (B7) and (B11), therefore this system has a globally stable, feasible coexistence equilibrium. Yet the interspecific coefficient A_{21} is larger in magnitude than

the sum of all the other coefficients taken together. The intra- versus interspecific competition argument is valid only for the geometric averages as in Eq. (B11), not for the individual coefficients themselves.

Finally, note that an alternative form of the Lotka–Volterra equations, preferred by Chesson (2000), reads

$$\frac{dn_i}{dt} = n_i b_i \left(1 + \sum_{j=1}^S \alpha_{ij} n_j \right), \quad (\text{B13})$$

where α_{ij} measures the effect of species j on species i 's intrinsic growth rate b_i . Eqs. (B3) and (B13) are both perfectly legitimate parameterizations, and can be transformed into one another by $A_{ij} = b_i \alpha_{ij}$. For $S = 2$, the feasibility condition Eq. (B7) reduces to $\alpha_{12}/\alpha_{22} < 1 < \alpha_{11}/\alpha_{21}$, implying $\alpha_{12} < \alpha_{22}$ and $\alpha_{21} < \alpha_{11}$. This yields a much more direct version of the principle that two species can only coexist if intraspecific effects exceed interspecific ones (Chesson 2000). Unfortunately, this more direct interpretation of the two-species coexistence rule via Eq. (B13) is only available in the two-species case. For $S > 3$, violating the condition does not preclude, and vice versa: fulfilling it does not ensure coexistence. Below we construct examples to show this. To make sure that our conclusions will hold in both the parameterizations of Eq. (B3) and Eq. (B13), we will deliberately set $b_i = 1$ for all i , making the two parameterizations equivalent.

B2.3 Three species

The only possible structurally stable dynamical behavior of the two-species competitive Lotka–Volterra model is the convergence to a stable fixed point. With three species, and still assuming purely competitive dynamics, limit cycles are also possible (May and Leonard 1975), but not chaos. Importantly, Eq. (B11), the familiar two-species condition between intra- and interspecific competition, no longer holds. In fact, one can construct counterexamples going both ways: competitive matrices where every pair of species satisfies the criterion and yet the system as a whole is unstable, and matrices where the criterion is violated yet coexistence is stable.

An example of the former is

$$\mathbf{b} = \begin{pmatrix} 1 \\ 1 \\ 1 \end{pmatrix}, \quad \mathbf{A} = - \begin{pmatrix} 10 & 9 & 5 \\ 9 & 10 & 9 \\ 5 & 9 & 10 \end{pmatrix}. \quad (\text{B14})$$

Since \mathbf{A} is symmetric, its eigenvalues determine the global stability of coexistence (MacArthur 1970), as discussed before. The eigenvalues are -5 and $(-25 \pm \sqrt{673})/2$, the largest of which is positive. Coexistence is therefore globally unstable: regardless of feasibility, the inevitable outcome is the extinction of at least one species (Figure B1, left panel). This is despite the fact that all species pairs individually satisfy the coexistence criteria, both in terms of Eq. (B3) and Eq. (B13), and so would stably coexist in the absence of the third species.

Similarly, let us consider the following parameterization:

$$\mathbf{b} = \begin{pmatrix} 1 \\ 1 \\ 1 \end{pmatrix}, \quad \mathbf{A} = - \begin{pmatrix} 10 & 7 & 12 \\ 15 & 10 & 8 \\ 7 & 11 & 10 \end{pmatrix}. \quad (\text{B15})$$

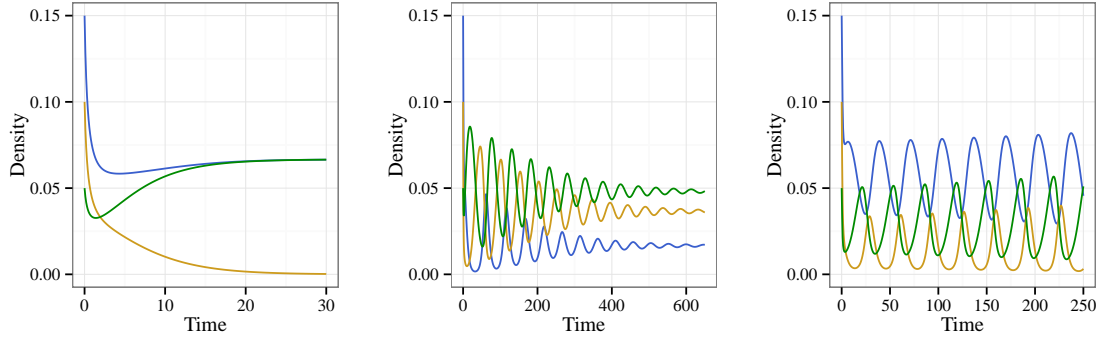


Figure B1: Dynamics of three-species competitive Lotka–Volterra equations. Left: intraspecific competition exceeds interspecific competition for all species pairs, yet there is no coexistence. Center: intraspecific competition does not exceed interspecific competition for all species pairs, yet coexistence is possible. Right: the coexistence equilibrium is unstable, but the species still coexist on a stable limit cycle.

Taking just species 1 and 2, the geometric mean of their interspecific competition coefficients exceeds that of the intraspecific ones. Also, $(b_2A_{21})/(b_1A_{11}) = \alpha_{21}/\alpha_{11} > 1$, violating two-species coexistence in the parameterization of Eq. (B13) as well. Yet the equilibrium densities are feasible: $\hat{\mathbf{n}} = -\mathbf{A}^{-1}\mathbf{b} = (10, 22, 29)/602$, and the eigenvalues of $\mathbf{J}|_{\hat{\mathbf{n}}} = \text{diag}(\hat{\mathbf{n}})\mathbf{A}$ are -1 and $(-2 \pm \sqrt{-1\sqrt{1591}})/301$, all of which have negative real parts. The coexistence equilibrium is therefore feasible and at least locally stable (Figure B1, center panel).

Finally, an example of a stable limit cycle solution is given by

$$\mathbf{b} = \begin{pmatrix} 1 \\ 1 \\ 1 \end{pmatrix}, \quad \mathbf{A} = -\begin{pmatrix} 10 & 6 & 12 \\ 14 & 10 & 2 \\ 8 & 18 & 10 \end{pmatrix} \quad (\text{B16})$$

(Figure B1, right panel).

B2.4 Four or more species

For four species, even purely competitive Lotka–Volterra dynamics may produce chaotic solutions. One example is given by

$$\mathbf{b} = \begin{pmatrix} 1.00 \\ 0.72 \\ 1.53 \\ 1.27 \end{pmatrix}, \quad \mathbf{A} = -\begin{pmatrix} 1.0000 & 1.0900 & 1.5200 & 0.0000 \\ 0.0000 & 0.7200 & 0.3168 & 0.9792 \\ 3.5649 & 0.0000 & 1.5300 & 0.7191 \\ 1.5367 & 0.6477 & 0.4445 & 1.2700 \end{pmatrix} \quad (\text{B17})$$

(after Vano et al. 2006); the dynamics is shown on Figure B2. For five or more species, a classic theorem by Smale (1976) establishes that one can construct the parameters of the competitive Lotka–Volterra equations to be compatible with *any* asymptotic dynamical behavior, i.e., the range of dynamics exhibited by these models is unrestricted.

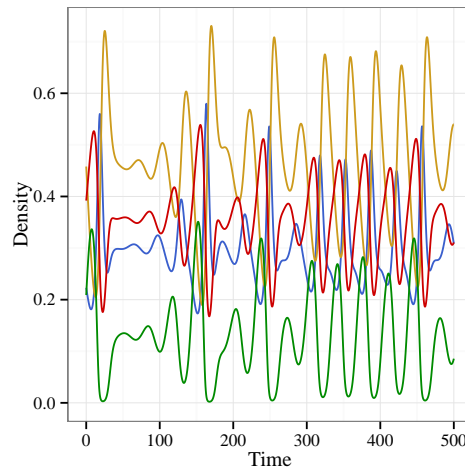


Figure B2: Chaos in a four-species competitive Lotka–Volterra system. The coexistence equilibrium is unstable, but the species still coexist on the stable chaotic attractor.

B2.5 Multispecies generalization of the two-species coexistence rule

Although the two-species coexistence rule does not apply in communities of more than two species, a generalization can be given for competitive matrices \mathbf{A} that are symmetric. This generalization is based on a simple corollary of Sylvester’s criterion.

Sylvester’s criterion for positive definite matrices (Horn and Johnson 2012) states that a real symmetric matrix \mathbf{A} has positive eigenvalues if and only if all its principal minors are positive (a “principal minor” of a square matrix \mathbf{A} is the determinant of a matrix obtained by deleting rows and columns of the same index from \mathbf{A}). Since \mathbf{A} has positive eigenvalues if and only if $-\mathbf{A}$ has negative ones, an immediate consequence of the above is Sylvester’s criterion for negative definite matrices: a real symmetric matrix has negative eigenvalues if and only if all its odd-sized principal minors are negative and all its even-sized principal minors are positive.

The set of all principal minors includes every 2×2 principal minor. Therefore a weaker but simpler version of Sylvester’s criterion for negative definite matrices states that all 2×2 principal minors must be positive for \mathbf{A} to have negative eigenvalues; i.e., failing to fulfill this criterion guarantees some nonnegative eigenvalues, but fulfilling it does not guarantee all negative ones.

In ecological terms, a 2×2 principal minor is simply the determinant of the interaction matrix of a two-species subsystem, with all other species absent. Requiring all 2×2 principal minors to be positive is therefore equivalent to requiring that all species pairs independently satisfy Eq. (B11). In this way, Sylvester’s criterion generalizes the two-species rule to multiple species: a community of S symmetrically competing species cannot be stable if there is even a single species pair violating the two-species coexistence rule.

B3 Decomposition of the interaction matrix

We decompose the interaction matrix \mathbf{A} , with coefficients $A_{ij} \leq 0$, as the sum of two matrices \mathbf{B} and \mathbf{C} , defined as

$$B_{ij} = \begin{cases} A_{ij} & \text{if } i \neq j, \\ 0 & \text{if } i = j, \end{cases} \quad (\text{B18})$$

$$C_{ij} = \begin{cases} 0 & \text{if } i \neq j, \\ A_{ij} & \text{if } i = j. \end{cases} \quad (\text{B19})$$

Thus, \mathbf{B} contains the interspecific effects, \mathbf{C} the intraspecific effects, and $\mathbf{A} = \mathbf{B} + \mathbf{C}$.

When \mathbf{A} is symmetric (and therefore both \mathbf{B} and \mathbf{C} are symmetric), it is simple to write bounds for the eigenvalues of \mathbf{A} in terms of the eigenvalues of \mathbf{B} and \mathbf{C} , and thus illustrate the effects on the stability of the system using the familiar language of intra- and interspecific competition.

The mathematical setting is as follows: take \mathbf{B} and \mathbf{C} symmetric, $S \times S$ matrices, and define $\mathbf{A} = \mathbf{B} + \mathbf{C}$. Because the matrices are symmetric, all eigenvalues are real. We number the eigenvalues in order: the eigenvalues of \mathbf{A} are $\alpha_1 \geq \alpha_2 \geq \dots \alpha_S$, those of \mathbf{B} are $\beta_1 \geq \beta_2 \geq \dots \beta_S$, and those of \mathbf{C} are $\gamma_1 \geq \gamma_2 \geq \dots \gamma_S$. Since every coefficient A_{ij} is negative or zero, it follows that all $\gamma_i \leq 0$, because the eigenvalues of \mathbf{C} are simply the coefficients on the diagonal of \mathbf{A} sorted in decreasing order. Also, since \mathbf{B} has all zeros along its diagonal, $\beta_1 \geq 0$ and $\beta_S \leq 0$. This is because the sum of the diagonal entries (zero in our case) is also the sum of all eigenvalues, so either every eigenvalue is zero, or some are positive and some are negative. For stability, we need $\alpha_1 < 0$.

When the matrices are symmetric, we can write the following inequalities (Horn and Johnson 2012):

$$\max_{i+j=S+k} \beta_i + \gamma_j \leq \alpha_k \leq \min_{i+j=k+1} \beta_i + \gamma_j, \quad (\text{B20})$$

where $k = 1, \dots, S$. Setting $k = 1$ (i.e., bounding α_1 , the rightmost eigenvalue of \mathbf{A} , determining stability), we can simplify the inequalities:

$$\max_j \beta_j + \gamma_{S-j+1} \leq \alpha_1 \leq \beta_1 + \gamma_1, \quad (\text{B21})$$

which implies

$$\beta_1 + \gamma_S \leq \alpha_1 \leq \beta_1 + \gamma_1. \quad (\text{B22})$$

These relationships allow us to write a *necessary* condition for stability:

$$\beta_1 + \gamma_S < 0, \quad (\text{B23})$$

meaning that the strongest self-regulation $\gamma_S = \min A_{ii}$ needs to be strong enough to offset the rightmost eigenvalue β_1 stemming from interspecific interactions. Similarly, we can write a *sufficient* condition for stability:

$$\beta_1 + \gamma_1 < 0, \quad (\text{B24})$$

meaning that the weakest self-regulation $\gamma_1 = \max A_{ii}$ needs to be strong enough to offset the rightmost eigenvalue β_1 stemming from interspecific interactions. For instance, in the two-species case, β_1 is simply equal to $-A_{12} = -A_{21}$. Assuming $A_{11} < A_{22}$ without loss of generality, $A_{11} < A_{12}$

is a necessary, while $A_{22} < A_{12}$ is a sufficient condition for two-species coexistence—consistently with the precise condition $A_{11}A_{22} > A_{12}^2$ coming from Eq. (B11).

Clearly, when the diagonal entries of \mathbf{A} are all equal, the two conditions are the same, providing a *necessary and sufficient* condition for stability.

How sharp are these bounds? Because we are foregoing the exact matrices \mathbf{B} and \mathbf{C} and only consider their eigenvalues, the bounds cannot be sharp in all cases. In fact, there are very many possible matrices having exactly the same eigenvalues (isospectral matrices). In particular, when we consider only the eigenvalues of \mathbf{C} , we forego the precise identity of the species, so that the $S!$ different ways of arranging the coefficients C_{ii} on the diagonal would yield exactly the same eigenvalues γ_i , but would alter the eigenvalues of \mathbf{A} . This subtle point is better understood through a simple example.

Take a given matrix \mathbf{B} , and suppose that the diagonal matrix \mathbf{C} has eigenvalues $\gamma_1 = -2$, $\gamma_2 = -9$, and $\gamma_3 = -10$. There are $3! = 6$ matrices \mathbf{C} with the same exact eigenvalues. However, each possible \mathbf{C} will yield a different $\mathbf{A} = \mathbf{B} + \mathbf{C}$ matrix, and thus different eigenvalues α_i . Table B1 shows that

C, B, and A			Eigenvalues	$\alpha_1 < 0$
$\begin{bmatrix} -2 & 0 & 0 \\ 0 & -9 & 0 \\ 0 & 0 & -10 \end{bmatrix}$	$\begin{bmatrix} 0 & -3 & -1 \\ -3 & 0 & -5 \\ -1 & -5 & 0 \end{bmatrix}$	$\begin{bmatrix} -2 & -3 & -1 \\ -3 & -9 & -5 \\ -1 & -5 & -10 \end{bmatrix}$	$\gamma_1 = -2, \gamma_2 = -9, \gamma_3 = -10$ $\beta_1 = 5.429, \beta_2 = 0.876, \beta_3 = -6.305$ $\alpha_1 = -0.792, \alpha_2 = -5.094, \alpha_3 = -15.114$	Yes
$\begin{bmatrix} -2 & 0 & 0 \\ 0 & -10 & 0 \\ 0 & 0 & -9 \end{bmatrix}$	$\begin{bmatrix} 0 & -3 & -1 \\ -3 & 0 & -5 \\ -1 & -5 & 0 \end{bmatrix}$	$\begin{bmatrix} -2 & -3 & -1 \\ -3 & -10 & -5 \\ -1 & -5 & -9 \end{bmatrix}$	$\gamma_1 = -2, \gamma_2 = -9, \gamma_3 = -10$ $\beta_1 = 5.429, \beta_2 = 0.876, \beta_3 = -6.305$ $\alpha_1 = -0.928, \alpha_2 = -4.903, \alpha_3 = -15.169$	Yes
$\begin{bmatrix} -9 & 0 & 0 \\ 0 & -2 & 0 \\ 0 & 0 & -10 \end{bmatrix}$	$\begin{bmatrix} 0 & -3 & -1 \\ -3 & 0 & -5 \\ -1 & -5 & 0 \end{bmatrix}$	$\begin{bmatrix} -9 & -3 & -1 \\ -3 & -2 & -5 \\ -1 & -5 & -10 \end{bmatrix}$	$\gamma_1 = -2, \gamma_2 = -9, \gamma_3 = -10$ $\beta_1 = 5.429, \beta_2 = 0.876, \beta_3 = -6.305$ $\alpha_1 = 0.941, \alpha_2 = -8.382, \alpha_3 = -13.559$	No
$\begin{bmatrix} -9 & 0 & 0 \\ 0 & -10 & 0 \\ 0 & 0 & -2 \end{bmatrix}$	$\begin{bmatrix} 0 & -3 & -1 \\ -3 & 0 & -5 \\ -1 & -5 & 0 \end{bmatrix}$	$\begin{bmatrix} -9 & -3 & -1 \\ -3 & -10 & -5 \\ -1 & -5 & -2 \end{bmatrix}$	$\gamma_1 = -2, \gamma_2 = -9, \gamma_3 = -10$ $\beta_1 = 5.429, \beta_2 = 0.876, \beta_3 = -6.305$ $\alpha_1 = 0.421, \alpha_2 = -7.148, \alpha_3 = -14.273$	No
$\begin{bmatrix} -10 & 0 & 0 \\ 0 & -2 & 0 \\ 0 & 0 & -9 \end{bmatrix}$	$\begin{bmatrix} 0 & -3 & -1 \\ -3 & 0 & -5 \\ -1 & -5 & 0 \end{bmatrix}$	$\begin{bmatrix} -10 & -3 & -1 \\ -3 & -2 & -5 \\ -1 & -5 & -9 \end{bmatrix}$	$\gamma_1 = -2, \gamma_2 = -9, \gamma_3 = -10$ $\beta_1 = 5.429, \beta_2 = 0.876, \beta_3 = -6.305$ $\alpha_1 = 1.057, \alpha_2 = -8.725, \alpha_3 = -13.333$	No
$\begin{bmatrix} -10 & 0 & 0 \\ 0 & -9 & 0 \\ 0 & 0 & -2 \end{bmatrix}$	$\begin{bmatrix} 0 & -3 & -1 \\ -3 & 0 & -5 \\ -1 & -5 & 0 \end{bmatrix}$	$\begin{bmatrix} -10 & -3 & -1 \\ -3 & -9 & -5 \\ -1 & -5 & -2 \end{bmatrix}$	$\gamma_1 = -2, \gamma_2 = -9, \gamma_3 = -10$ $\beta_1 = 5.429, \beta_2 = 0.876, \beta_3 = -6.305$ $\alpha_1 = 0.629, \alpha_2 = -7.597, \alpha_3 = -14.032$	No

Table B1: Eigenvalues of $\mathbf{C} + \mathbf{B} = \mathbf{A}$, as a function of the ordering of the diagonal entries of \mathbf{C} . The same set of coefficients produce different eigenvalues and stability properties for \mathbf{A} depending on the ordering, despite the fact that the eigenvalues of the two constituent matrices \mathbf{C} and \mathbf{B} are unchanged by this rearrangement.

for the very same eigenvalues of \mathbf{B} and \mathbf{C} , we can obtain α_1 as low as -0.928 , or as high as 1.057 . This is reflected in the bounds introduced above:

$$\beta_1 + \gamma_S = 5.429 - 10 = -4.571 \leq \alpha_1 \leq \beta_1 + \gamma_1 = 5.429 - 2 = 3.429. \quad (\text{B25})$$

B4 Random matrices

B4.1 Symmetric matrices

Let \mathbf{A} be an $S \times S$ matrix, constructed as follows. Each diagonal entry is set to zero. Then each upper triangular entry is drawn from some probability distribution with mean zero, variance V , and all moments finite. Finally, each lower triangular entry A_{ij} is set equal to A_{ji} , making \mathbf{A} symmetric.

Matrices constructed this way are called *Wigner matrices*. Consider now the matrix \mathbf{A}/\sqrt{SV} . Since it is symmetric, all eigenvalues are real. Their empirical spectral distribution, in the limit of large S , follows the *Wigner semicircle distribution*:

$$\tilde{f}(x) = \frac{\sqrt{4-x^2}}{2\pi}, \quad -2 \leq x \leq 2 \quad (\text{B26})$$

and 0 otherwise, where x represents the position along the real line where the eigenvalues may fall (Bai and Silverstein 2009, Allesina and Tang 2015). The most important property of this distribution is its *universality*: any underlying distribution from which the matrix entries are drawn will lead to $\tilde{f}(x)$ as $S \rightarrow \infty$; the only constraint is a zero mean and finite higher moments. For finite S , one can approximate the above distribution for \mathbf{A} instead of \mathbf{A}/\sqrt{SV} as

$$f(x) \approx \frac{\sqrt{4SV-x^2}}{2\pi SV}, \quad -2\sqrt{SV} \leq x \leq 2\sqrt{SV} \quad (\text{B27})$$

and 0 otherwise, where the approximation improves with increasing S . See the left panel of Figure B3 for an example.

The requirement that all diagonal entries are zero can be relaxed. Assume the diagonal entries have mean zero and variance V_d . By definition,

$$V_d = \frac{1}{S} \sum_{i=1}^S (A^2)_{ii}, \quad (\text{B28})$$

where $(A^2)_{ij}$ is the (i, j) th entry of $\mathbf{A}\mathbf{A} = \mathbf{A}^2$. The variance of all matrix entries may then be written

$$\frac{1}{S^2} \sum_{i=1}^S \sum_{j=1}^S (A^2)_{ij} = \frac{1}{S^2} \sum_{i=1}^S (A^2)_{ii} + \frac{1}{S(S-1)} \sum_{i=1}^S \sum_{j \neq i}^S (A^2)_{ij} = \frac{V_d}{S} + V. \quad (\text{B29})$$

In other words, as long as V_d does not scale with S for some reason, the contribution of the diagonal entries' variance to the total variance will be negligible in the large S limit, and only the offdiagonal variance V matters. Adding diagonal variance to a large Wigner matrix therefore leaves its spectral properties unchanged.

What happens if the diagonal entries have a nonzero mean, say, μ_d ? (The mean of the offdiagonal entries is still assumed to be zero.) Let \mathbf{I} be the $S \times S$ identity matrix; \mathbf{A} can then be written as $\mathbf{A} = (\mathbf{A} - \mu_d \mathbf{I}) + \mu_d \mathbf{I}$. The matrix $(\mathbf{A} - \mu_d \mathbf{I})$ has zero mean diagonal, therefore it is a Wigner matrix for which our previous results hold. When adding the diagonal matrix $\mu_d \mathbf{I}$ to this, μ_d is simply added to each eigenvalue.² The eigenvalue distribution in the large S limit therefore reads

$$f(x) = \frac{\sqrt{4SV - (x - \mu_d)^2}}{2\pi SV}, \quad -2\sqrt{SV} \leq x - \mu_d \leq 2\sqrt{SV} \quad (\text{B30})$$

²The eigenvalues of \mathbf{A} are, by definition, numbers λ satisfying $\det(\mathbf{A} - \lambda \mathbf{I}) = 0$. The eigenvalues of $\mathbf{A} + \mu_d \mathbf{I}$ are numbers λ' satisfying $\det(\mathbf{A} + \mu_d \mathbf{I} - \lambda' \mathbf{I}) = \det(\mathbf{A} - (\lambda' - \mu_d) \mathbf{I}) = 0$. Therefore $\lambda = \lambda' - \mu_d$, or $\lambda' = \lambda + \mu_d$.

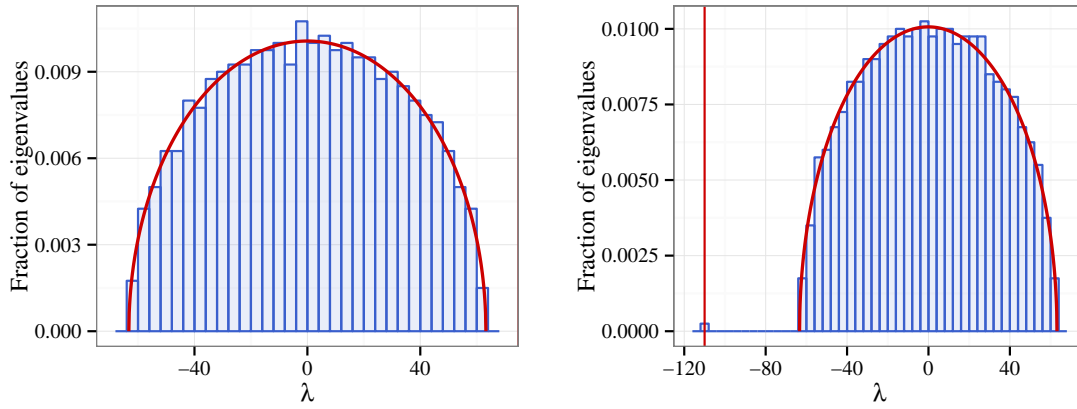


Figure B3: Left panel: eigenvalue distribution (blue histogram) of a Wigner random matrix with $S = 1000$, $V = 1$, and the entries drawn from a normal distribution. The red curve is the analytical prediction of Eq. (B27). Right panel: eigenvalue distribution (blue histogram) of a symmetric random matrix with $S = 1000$, $\mu = -1/10$, $V = 1$, $\mu_d = 0$, $V_d = 1$, and all entries drawn from a normal distribution. The red curve is the analytical prediction based on Eq. (B32); the single outlier eigenvalue is predicted to be at $S\mu + V/\mu = -110$. Notice also that the variance of the diagonal entries is as large as the offdiagonal variance, yet this has no discernible effect on the eigenvalue distribution (the red semicircle's prediction is still almost perfect).

and 0 otherwise.

Finally, one can consider the case when the offdiagonal entries also have a nonzero mean μ . Let \mathbf{E} be the $S \times S$ matrix with all entries equal to one; then we can write

$$\mathbf{A} = (\mathbf{A} - \mu_d \mathbf{I} - \mu \mathbf{E} + \mu \mathbf{I}) + \mu_d \mathbf{I} + \mu \mathbf{E} - \mu \mathbf{I}. \quad (\text{B31})$$

In the parentheses, we first shift the diagonal to have zero mean, then we shift the matrix so that its offdiagonal entries have zero mean, but in the process also affect the diagonal—the final term restores it back to have zero mean. The matrix in parentheses is therefore a Wigner matrix, its eigenvalue distribution given by the Wigner semicircle distribution. The matrix $\mu_d \mathbf{I} - \mu \mathbf{I} = (\mu_d - \mu) \mathbf{I}$ simply adds $\mu_d - \mu$ to each eigenvalue. Finally, note that \mathbf{E} can be written as the outer product of the vector $(1, 1, \dots, 1)$ (a vector of all ones) with itself—that is, \mathbf{E} is a rank-one matrix. According to the theory of low-rank perturbations to random matrices (O'Rourke and Renfrew 2014), the effect of adding $\mu \mathbf{E}$ is to make one single eigenvalue assume the value $S\mu + V/\mu$ (for S large, the second term is negligible).³ The shape of the rest of the eigenvalue distribution remains unchanged. The final form of the empirical spectral distribution for a symmetric random matrix with offdiagonal mean and variance μ , V and diagonal mean and variance μ_d , V_d therefore reads

$$f(x) = \frac{\sqrt{4SV - (x - \mu_d + \mu)^2}}{2\pi SV}, \quad -2\sqrt{SV} \leq x - \mu_d + \mu \leq 2\sqrt{SV} \quad (\text{B32})$$

³Technical conditions hold on whether the V/μ term is actually present (see O'Rourke and Renfrew 2014); in essence, this term will be there as long as μ is large enough to make the single modified eigenvalue isolated from the rest of the distribution. See the right panel of Figure B3 for an example.

and 0 otherwise, except for a single outlier eigenvalue equal to $S\mu + V/\mu$ (with the V/μ term missing if μ is too small). See the right panel of Figure B3 for an example.

B4.2 Nonsymmetric matrices

The Wigner semicircle distribution holds only for symmetric random matrices. More generally, one may consider the nonsymmetric random matrix \mathbf{A} , constructed as follows. First, each diagonal entry is set to zero. Then each pair of entries (A_{ij}, A_{ji}) are sampled from a bivariate distribution with zero marginal means, marginal variances $V < \infty$, and pairwise correlation ρ . All moments of the bivariate distribution are assumed finite.

Matrices constructed this way are called *elliptic matrices*. According to the *elliptic law* (Sommers et al. 1998, O'Rourke and Renfrew 2014), the eigenvalues of \mathbf{A}/\sqrt{SV} are uniformly distributed in an ellipse in the complex plane, with horizontal and vertical semiaxes $1 \pm \rho$. For finite but large S , the eigenvalues of \mathbf{A} are distributed uniformly in an ellipse with horizontal/vertical semiaxes $\sqrt{SV}(1 \pm \rho)$ (Figure B4, left panel). Just as in the symmetric case, the elliptic law is universal: *any* bivariate distribution with the same marginal variances and correlation will result in the eigenvalues being distributed in the same ellipse.

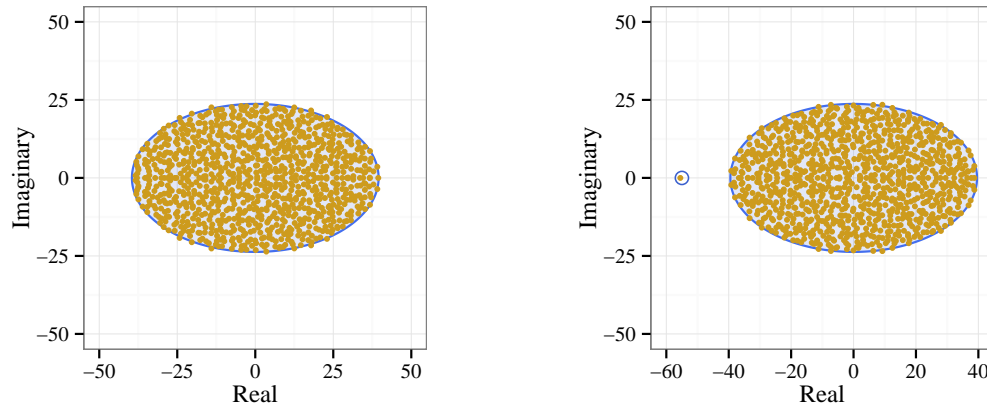


Figure B4: Left panel: eigenvalues (yellow points) of an elliptic random matrix with $S = 1000$, and all pairs (A_{ij}, A_{ji}) sampled from a bivariate normal distribution with $\mu = 0$, $V = 1$, and $\rho = 1/4$. The blue ellipse is the analytical prediction for the region where the eigenvalues are uniformly distributed. Right panel: eigenvalues (yellow points) of an elliptic random matrix with $S = 1000$, and all pairs (A_{ij}, A_{ji}) sampled from a bivariate normal distribution with $\mu = -1/20$, $V = 1$, and $\rho = 1/4$. The blue ellipse and circle are the analytical prediction; the single outlying eigenvalue is predicted to be at $S\mu + \rho V/\mu = -55$.

The generalizations that we performed in the symmetric case carry over to the nonsymmetric case as well, as there is nothing in these generalizations that is specific to Wigner matrices. Therefore, if the bivariate distribution has mean μ , and the diagonal entries have mean μ_d and variance V_d , the eigenvalues will be uniformly distributed in an ellipse with horizontal/vertical semiaxes $\sqrt{SV}(1 \pm \rho)$ centered at $(\mu_d - \mu, 0)$ in the complex plane, and there will be a single outlying eigenvalue at $S\mu + \rho V/\mu$ (the second term is zero if μ is too small). See the right panel of Figure B4 for an

B5 Maximizing/minimizing the rightmost eigenvalue

The source code and documentation for an implementation of this algorithm, written in C, can be downloaded from <https://github.com/dysordys/intra-inter>. For reference, we also provide the code listing right here.

[illegible]

```

8 #include <stdio.h>
9 #include <string.h>
10 #include <math.h>
11
12 // Matrices, vectors, eigenvalues
13 #include <gsl/gsl_math.h>
14 #include <gsl/gsl_vector.h>
15 #include <gsl/gsl_matrix.h>
16 #include <gsl/gsl_eigen.h>
17 #include <gsl/gsl_sort_vector.h>
18 #include <gsl/gsl_blas.h>
19
20 // Random number generation and random distributions
21 #include <gsl/gsl_rng.h>
22 #include <gsl/gsl_randist.h>
23
24 // Set multiplier for eigenvalues to increase difference
25 #define EIGMULT 10.0
26
27 // Global variables
28 int n;
29 int npairs;
30 gsl_vector * eval;
31 gsl_matrix * M;
32 gsl_matrix * A;
33 gsl_vector * diagonal;
34 gsl_matrix * pairs;
35 gsl_matrix * indices;
36 gsl_eigen_symm_workspace * w;
37
38
39 //////////////// Functions for reading/writing matrices ////////////////
40 // read a matrix stored in filename and assign to M
41 // M is initialized in the process
42 gsl_matrix * read_matrix(int n,
43     char * filename){
44     gsl_matrix * M = gsl_matrix_calloc(n, n);
45     FILE * F;
46     F = fopen(filename, "rb");
47     gsl_matrix_fscanf(F, M);
48     fclose(F);
49     return M;
50 }
51
52 int initialize_structures(char * filename){
53     M = gsl_matrix_calloc(n, n);
54     FILE * F;
55     F = fopen(filename, "rb");
56     gsl_matrix_fscanf(F, M);
57     fclose(F);
58
59     // Now initialize all the variables needed for the eigenvalue search
60     npairs = n * (n - 1) / 2;
61     A = gsl_matrix_calloc(n, n);
62     eval = gsl_vector_alloc(n);

```

```

63     w = gsl_eigen_symm_alloc(n);
64     pairs = gsl_matrix_calloc(npairs, 2);
65     indices = gsl_matrix_calloc(npairs, 2);
66     diagonal = gsl_vector_calloc(n);
67     int i, j, k;
68     k = 0;
69     for (i = 0; i < n; i++){
70         for (j = i; j < n; j++){
71             if (j == i){
72                 gsl_vector_set(diagonal, j, gsl_matrix_get(M, j, j));
73             }
74             else {
75                 gsl_matrix_set(pairs, k, 0, gsl_matrix_get(M, i, j));
76                 gsl_matrix_set(pairs, k, 1, gsl_matrix_get(M, j, i));
77                 gsl_matrix_set(indices, k, 0, i);
78                 gsl_matrix_set(indices, k, 1, j);
79                 k++;
80             }
81         }
82     }
83     return 0;
84 }
85
86 int free_structures(){
87     gsl_matrix_free(M);
88     gsl_matrix_free(A);
89     gsl_matrix_free(pairs);
90     gsl_matrix_free(indices);
91     gsl_vector_free(diagonal);
92     gsl_vector_free(eval);
93     gsl_eigen_symm_free(w);
94     return 0;
95 }
96
97 // print a matrix either to a file or to a stream
98 int print_matrix(FILE * F,
99                 gsl_matrix * M){
100     int i, j;
101     for (i = 0; i < n; i++){
102         for (j = 0; j < n; j++){
103             fprintf(F, "%f ", gsl_matrix_get(M, i, j));
104         }
105         fprintf(F, "\n");
106     }
107     return 0;
108 }
109
110 ////////////////////////////////////////////////// Functions for random numbers //////////////////////////////////////////
111 int random_setup(gsl_rng ** r, int seed){
112     const gsl_rng_type * T;
113     gsl_rng_env_setup();
114     T = gsl_rng_default;
115     *r = gsl_rng_alloc(T);
116     gsl_rng_set (*r, seed);
117     return 0;

```



```

118 }
119
120 int random_free(gsl_rng ** r){
121     gsl_rng_free(*r);
122     return 0;
123 }
124
125 ////////////////////////////////////////////////// Functions for mutating matrices ///////////////////////////////////
126 // Mutate the matrix M by swapping two coefficients in the
127 // upper-triangular part and the corresponding lower-triangular
128 // coefficients as well, to keep symmetry
129 int mutate_off_diagonal(int n,
130                         gsl_rng * r,
131                         gsl_matrix * M){
132     int i = gsl_rng_uniform_int(r, n);
133     int j = gsl_rng_uniform_int(r, n);
134     while(j == i){
135         j = gsl_rng_uniform_int(r, n);
136     }
137     int k = gsl_rng_uniform_int(r, n);
138     int l = gsl_rng_uniform_int(r, n);
139     while(k == l){
140         l = gsl_rng_uniform_int(r, n);
141     }
142     double tmp;
143     tmp = gsl_matrix_get(M, i, j);
144     gsl_matrix_set(M, i, j, gsl_matrix_get(M, k, l));
145     gsl_matrix_set(M, k, l, tmp);
146
147     tmp = gsl_matrix_get(M, j, i);
148     gsl_matrix_set(M, j, i, gsl_matrix_get(M, l, k));
149     gsl_matrix_set(M, l, k, tmp);
150     return 0;
151 }
152
153 // Mutate by swapping two elements on the diagonal
154 int mutate_diagonal(int n,
155                     gsl_rng * r,
156                     gsl_matrix * M){
157
158     int i = gsl_rng_uniform_int(r, n);
159     int j = i;
160     while(j == i){
161         j = gsl_rng_uniform_int(r, n);
162     }
163     double tmp;
164     tmp = gsl_matrix_get(M, i, i);
165     gsl_matrix_set(M, i, i, gsl_matrix_get(M, j, j));
166     gsl_matrix_set(M, j, j, tmp);
167     return 0;
168 }
169
170 ////////////////////////////////////////////////// Functions for calculating eigenvalues ///////////////////////////////////
171 // Setup the environment for computing the eigenvalues
172 int eigenvalues_setup(int n,

```

```

173         gsl_matrix ** tmpM,
174         gsl_vector ** eval,
175         gsl_eigen_symm_workspace ** w){
176 // Allocate temporary matrix for calculations
177 *tmpM = gsl_matrix_calloc(n, n);
178 // Allocate vector for storing eigenvalues
179 *eval = gsl_vector_calloc(n);
180 // Allocate workspace for eigenvalue calculation
181 *w = gsl_eigen_symm_alloc(n);
182 return 0;
183 }
184
185 // Free memory associated with eigenvalues
186 int eigenvalues_free(gsl_matrix ** tmpM,
187                     gsl_vector ** eval,
188                     gsl_eigen_symm_workspace ** w){
189     gsl_matrix_free(*tmpM);
190     gsl_vector_free(*eval);
191     gsl_eigen_symm_free(*w);
192     return 0;
193 }
194
195 // Find the largest eigenvalue of the symmetric matrix M
196 double find_max_eigen(gsl_matrix * M,
197                      gsl_matrix * tmpM,
198                      gsl_vector * eval,
199                      gsl_eigen_symm_workspace * w){
200 // Copy the matrix M, as it will be destroyed
201 gsl_matrix_memcpy(tmpM, M);
202 // Find the eigenvalues
203 gsl_eigen_symm(tmpM, eval, w);
204 // return the maximum eigenvalue
205 return gsl_vector_max(eval);
206 }
207
208 int build_A(gsl_vector * solution, gsl_vector * diag){
209 // build matrix A
210 int i;
211 gsl_matrix_set_zero(A);
212 for (i = 0; i < npairs; i++){
213     gsl_matrix_set(A, gsl_matrix_get(indices, gsl_vector_get(solution, i), 0),
214                   gsl_matrix_get(indices, gsl_vector_get(solution, i), 1),
215                   gsl_matrix_get(pairs, i, 1));
216     gsl_matrix_set(A, gsl_matrix_get(indices, gsl_vector_get(solution, i), 1),
217                   gsl_matrix_get(indices, gsl_vector_get(solution, i), 0),
218                   gsl_matrix_get(pairs, i, 0));
219 }
220 for (i = 0; i < n; i++){
221     gsl_matrix_set(A, i, i, gsl_vector_get(diag, i));
222 }
223 return 0;
224 }
225
226 double find_leading_eigen(gsl_vector * solution, gsl_vector * diag){
227     build_A(solution, diag);

```

```

228     // always find the eigenvalues of A;
229     // it is destroyed by the operation
230     gsl_eigen_symm(A, eval, w);
231     // return the maximum eigenvalue
232     return gsl_vector_max(eval);
233 }
234
235 ////////////////////////////////////////////////// Functions to Run Search Algorithms ///////////////////////////////////
236 int GeneticAlgorithm (int n,           // number of species
237                      char * filename, // file storing the matrix
238                      int seed,
239                      int maximize,
240                      int npop,
241                      int ngen,
242                      int BvsC){ // 1 for offdiagonal optimization, 0 for diagonal
243     int i = 0;
244     // initialize structures
245     fprintf(stderr, "Initializing\n");
246     i = initialize_structures(filename);
247
248     gsl_rng * r = NULL;
249     i = random_setup(&r, seed);
250
251     if (maximize == 1) {
252         fprintf(stderr, "GA to Maximize\n");
253     }
254     else if (maximize == -1) {
255         fprintf(stderr, "GA to Minimize\n");
256     }
257     gsl_vector * bestsol = gsl_vector_calloc(npairs);
258     gsl_vector * bestdiag = gsl_vector_calloc(n);
259     double bestfit = 0.0;
260
261     for (i = 0; i < npairs; i++){
262         gsl_vector_set(bestsol, i, i);
263     }
264     gsl_vector_memcpy(bestdiag, diagonal);
265
266     bestfit = maximize * find_leading_eigen(bestsol, bestdiag);
267     fprintf(stderr, "Original Matrix: %f\n", maximize * bestfit);
268
269     gsl_vector * popsol[npop];
270     gsl_vector * popdiag[npop];
271     gsl_vector * pop2sol[npop];
272     gsl_vector * pop2diag[npop];
273
274     // initialize populations
275     for (i = 0; i < npop; i++){
276         popsol[i] = gsl_vector_calloc(npairs);
277         popdiag[i] = gsl_vector_calloc(n);
278
279         pop2sol[i] = gsl_vector_calloc(npairs);
280         pop2diag[i] = gsl_vector_calloc(n);
281
282         gsl_vector_memcpy(popsol[i], bestsol);

```

```

283         gsl_vector_memcpy(popdiag[i], bestdiag);
284
285         gsl_rng_shuffle(r, popsol[i]->data, n, sizeof (double));
286         gsl_rng_shuffle(r, popdiag[i]->data, n, sizeof (double));
287     }
288
289     gsl_vector * fitness = gsl_vector_calloc(npop);
290     int j, dad, mom, k1, k2;
291     double tmp;
292     for (i = 0; i < ngen; i++){
293         // compute fitness and save best sol
294         for (j = 0; j < npop; j++){
295             tmp = maximize * find_leading_eigen(popsol[j], popdiag[j]);
296             gsl_vector_set(fitness, j, tmp);
297             if (tmp > bestfit){
298                 bestfit = tmp;
299                 if (BvsC == 1){
300                     gsl_vector_memcpy(bestsol, popsol[j]);
301                 }
302                 else {
303                     gsl_vector_memcpy(bestdiag, popdiag[j]);
304                 }
305                 fprintf(stderr, "%d %f\n", i, maximize * bestfit);
306             }
307         }
308         // reproduce
309         for (j = 0; j < npop; j++){
310             if (j < 50){
311                 if (BvsC == 1){
312                     gsl_vector_memcpy(pop2sol[j], bestsol);
313                 }
314                 else {
315                     gsl_vector_memcpy(pop2diag[j], bestdiag);
316                 }
317             }
318             else{
319                 dad = gsl_rng_uniform_int(r, npop);
320                 mom = gsl_rng_uniform_int(r, npop);
321                 if (gsl_vector_get(fitness, dad) > gsl_vector_get(fitness, mom)){
322                     if (BvsC == 1){
323                         gsl_vector_memcpy(pop2sol[j], popsol[dad]);
324                     }
325                     else {
326                         gsl_vector_memcpy(pop2diag[j], popdiag[dad]);
327                     }
328                 }
329                 else {
330                     if (BvsC == 1){
331                         gsl_vector_memcpy(pop2sol[j], popsol[mom]);
332                     }
333                     else {
334                         gsl_vector_memcpy(pop2diag[j], popdiag[mom]);
335                     }
336                 }
337             }

```

```

338         // mutation
339         if (BvsC == 1){
340             k1 = gsl_rng_uniform_int(r, npairs);
341             k2 = gsl_rng_uniform_int(r, npairs);
342             while (k1 == k2) {
343                 k2 = gsl_rng_uniform_int(r, npairs);
344             }
345             tmp = gsl_vector_get(pop2sol[j], k1);
346             gsl_vector_set(pop2sol[j], k1, gsl_vector_get(pop2sol[j], k2));
347             gsl_vector_set(pop2sol[j], k2, tmp);
348         }
349         else {
350             k1 = gsl_rng_uniform_int(r, n);
351             k2 = gsl_rng_uniform_int(r, n);
352             while (k1 == k2) {
353                 k2 = gsl_rng_uniform_int(r, n);
354             }
355             tmp = gsl_vector_get(pop2diag[j], k1);
356             gsl_vector_set(pop2diag[j], k1, gsl_vector_get(pop2diag[j], k2));
357             gsl_vector_set(pop2diag[j], k2, tmp);
358         }
359     }
360     // copy over
361     for (j = 0; j < npop; j++){
362         if (BvsC == 1){
363             gsl_vector_memcpy(popsol[j], pop2sol[j]);
364         }
365         else {
366             gsl_vector_memcpy(popdiag[j], pop2diag[j]);
367         }
368     }
369 }
370
371
372 FILE * F;
373 char OutFileName[1000];
374 if (BvsC == 1) {
375     if (maximize == 1){
376         sprintf(OutFileName, "%s.Bmax--%d", filename, seed);
377     }
378     if (maximize == -1){
379         sprintf(OutFileName, "%s.Bmin--%d", filename, seed);
380     }
381 } else {
382     if (maximize == 1){
383         sprintf(OutFileName, "%s.max--%d", filename, seed);
384     }
385     if (maximize == -1){
386         sprintf(OutFileName, "%s.min--%d", filename, seed);
387     }
388 }
389 F = fopen(OutFileName, "wb");
390 build_A(bestsol, bestdiag);
391 print_matrix(F, A);
392 fclose(F);

```

```

393
394     gsl_vector_free(bestsol);
395
396     for (i = 0; i < npop; i++){
397         gsl_vector_free(popsol[i]);
398         gsl_vector_free(pop2sol[i]);
399     }
400     gsl_vector_free(fitness);
401
402     free_structures();
403     random_free(&r);
404     return 0;
405 }
406
407 // Hill-climber with multiple sampling at each step to find the matrix structure
408 // that maximizes or minimizes the leading eigenvalue
409 int HillClimb (int n,           // number of species
410               char * filename, // file storing the matrix
411               int num_steps,   // number of steps without improvement before quitting
412               int num_try,     // number of solutions to try at each step
413               int seed,        // random seed
414               int maximize,    // 1 to maximize, -1 to minimize
415               int BvsC){       // mutate diagonal (0) or off-diagonal (1)
416     int i = 0;
417     double fit = 0.0;
418
419     // read in the matrix
420     gsl_matrix * M = NULL;
421     M = read_matrix(n, filename);
422
423     // initialize the random number generator
424     gsl_rng * r = NULL;
425     i = random_setup(&r, seed);
426
427     // setup eigenvalues
428     gsl_matrix * tmpM = NULL; // temporary matrix for eigenvalue calculation
429     gsl_vector * eval = NULL; // vector for storing eigenvalues
430     gsl_eigen_symm_workspace * w = NULL; // workspace for eigenvalues
431     i = eigenvalues_setup(n, &tmpM, &eval, &w);
432
433     // SPECIFIC TO HC
434     fprintf(stderr, "starting HC of leading eigenvalue with %d steps, %d tries per step\n",
435             num_steps, num_try);
436
437     gsl_matrix * M1 = gsl_matrix_calloc(n, n);
438     gsl_matrix * M2 = gsl_matrix_calloc(n, n);
439
440     fit = find_max_eigen(M, tmpM, eval, w);
441
442     double fit1 = fit;
443     double fit2 = fit;
444
445     int how_many_steps = 0;
446     int counter = 0;

```

```

447 while(how_many_steps < num_steps){
448     counter++;
449     how_many_steps++;
450     gsl_matrix_memcpy(M1, M);
451     fit1 = fit;
452     // now mutate several times and save the best
453     for (i = 0; i < num_try; i++){
454         gsl_matrix_memcpy(M2, M);
455         if (BvsC == 1){
456             mutate_off_diagonal(n, r, M2);
457         }
458         else {
459             mutate_diagonal(n, r, M2);
460         }
461         fit2 = find_max_eigen(M2, tmpM, eval, w);
462         if ((fit1 - fit2) * maximize < 0){
463             // we have a better solution
464             fit1 = fit2;
465             gsl_matrix_memcpy(M1, M2);
466         }
467     }
468     if ((fit - fit1) * maximize < 0){
469         // accept the move
470         fit = fit1;
471         gsl_matrix_memcpy(M, M1);
472         how_many_steps = 0;
473         fprintf(stderr, "step %d -- new best solution: %.6f\n", counter, fit);
474     }
475     else if ((counter % 1000) == 0){
476         fprintf(stderr, "step %d\n", counter);
477     }
478 }
479
480 gsl_matrix_free(M1);
481 gsl_matrix_free(M2);
482
483 // END SPECIFIC TO HC
484
485 // Stuff for output
486 char OutFileName[1000];
487 char FileNameRoot[1000];
488 char *dotBm;
489 strcpy(FileNameRoot, filename);
490 dotBm = strrchr(FileNameRoot, '.');
491 *dotBm = '\0';
492 // Save the results
493 if (maximize == 1) {
494     if (BvsC == 1) {
495         sprintf(OutFileName, "%s.Bmax--%d", FileNameRoot, seed);
496     }
497     else{
498         sprintf(OutFileName, "%s.max--%d", FileNameRoot, seed);
499     }
500 }
501 } else if (maximize == -1) {

```

```

502         if (BvsC == 1) {
503             sprintf(OutFileName,"%s.Bmin--%d", FileNameRoot, seed);
504         }
505         else{
506             sprintf(OutFileName,"%s.min--%d", FileNameRoot, seed);
507         }
508     }
509
510     int l, m;
511     FILE * F = fopen(OutFileName,"w");
512     for (l = 0; l < n; l++){
513         for (m = 0; m < n; m++){
514             fprintf(F, "%f ", gsl_matrix_get(M, l, m));
515         }
516         fprintf(F, "\n");
517     }
518     fclose(F);
519     // free matrix M
520     gsl_matrix_free(M);
521     // free eigenvalue-related variables
522     i = eigenvalues_free(&tmpM, &eval, &w);
523     // free random number generator
524     i = random_free(&r);
525     return 0;
526 }
527
528
529 int main (int argc, char *argv[]){
530     n = atoi(argv[1]);          // number of species
531     char * filename = argv[2];  // file storing the matrix
532     int seed = atoi(argv[3]);   // seed for random number generator
533     int maximize = atoi(argv[4]); // are we maximizing (1) or minimizing (-1)?
534     int para1 = atoi(argv[5]);  // first parameter for search algorithm
535     int para2 = atoi(argv[6]);  // second parameter for search algorithm
536     int BvsC = atoi(argv[7]);   // what are we mutating? 1 for offdiagonal, 0 for
                                // diagonal
537     int SearchAlg = atoi(argv[8]); // Genetic algorithm (1) or Hill climber (2)?
538
539     if (SearchAlg == 1) {
540         GeneticAlgorithm (n, filename, seed, maximize, para1, para2, BvsC);
541     }
542     else if (SearchAlg == 2) {
543         HillClimb (n, filename, para1, para2, seed, maximize, BvsC);
544     }
545     return(0);
546 }

```

B6 Explaining the pattern of intraspecific interactions leading to the largest and smallest rightmost eigenvalue

Here we show that the patterns of intraspecific coefficients on Figure 1 of the main text are generic and expected to hold in all cases, except when the variance V_d of the diagonal entries is large. As

explained in Section B3, \mathbf{A} is the interaction matrix, decomposed as $\mathbf{A} = \mathbf{B} + \mathbf{C}$, where \mathbf{B} is the matrix of interspecific and \mathbf{C} the diagonal matrix of intraspecific effects. The rightmost eigenvalue of \mathbf{A} is α_1 , and that of \mathbf{B} is β_1 . Summarizing the patterns of \mathbf{C} 's diagonal entries to be explained (Figure 1 in main text):

1. $(\max \beta_1, \max \alpha_1)$: The strength (absolute value) of the diagonal entries first increases, then decreases, approximately forming a V-shape.
2. $(\max \beta_1, \min \alpha_1)$: The strength of the diagonal entries first decreases, then increases, approximately forming an upside-down V-shape.
3. $(\text{random } \beta_1, \max \alpha_1)$: The strength of the diagonal entries first increases, then decreases, approximately forming a V-shape. This V-shape is less pronounced, “fuzzier”, than in the maximum β_1 case.
4. $(\text{random } \beta_1, \min \alpha_1)$: The strength of the diagonal entries first decreases, then increases, approximately forming an upside-down V-shape. This upside-down V-shape is less pronounced than in the maximum β_1 case.
5. $(\min \beta_1, \max \alpha_1)$: The strength of the diagonal entries increases monotonically with the variance of the corresponding species' interspecific coefficients. That is, species 1 will have the strongest and species S the weakest intraspecific coefficient, provided that the variance of the offdiagonal entries is largest in the first row and smallest in the S th.
6. $(\min \beta_1, \min \alpha_1)$: The strength of the diagonal entries roughly decreases with the variance of the corresponding species' interspecific coefficients, but this decrease is not necessarily strict or monotonic.

These patterns can be explained via standard eigenvalue sensitivity theory. We have $\mathbf{A} = \mathbf{B} + \mathbf{C}$. Let us write \mathbf{C} as the mean intraspecific interaction μ_d plus the deviation from the mean: $\mathbf{C} = (\mathbf{C} - \mu_d \mathbf{I}) + \mu_d \mathbf{I}$, where \mathbf{I} is the identity matrix. With the notation $\Delta \mathbf{C} = \mathbf{C} - \mu_d \mathbf{I}$, we have $\mathbf{A} = \mathbf{B} + \mu_d \mathbf{I} + \Delta \mathbf{C}$. The eigenvalues of $\mathbf{B} + \mu_d \mathbf{I}$ are the eigenvalues of \mathbf{B} plus μ_d (see Section B4), and the eigenvectors remain unchanged. We therefore only need to determine the effect of $\Delta \mathbf{C}$ to obtain α_1 . This we can do, to a first-order approximation, by writing the eigenvalues of \mathbf{A} as those of $\mathbf{B} + \mu_d \mathbf{I}$ plus a correction imposed by the perturbing matrix $\Delta \mathbf{C}$:

$$\alpha_1 \approx (\beta_1 + \mu_d) + \mathbf{w} \Delta \mathbf{C} \mathbf{w}, \quad (\text{B33})$$

where \mathbf{w} is the eigenvector corresponding to α_1 . Here we used the general sensitivity formula for eigenvalues (e.g., Caswell 2001, chapter 9); note that, because \mathbf{B} is symmetric, the left and right eigenvectors are identical. Since \mathbf{C} is diagonal, the product $\mathbf{w} \Delta \mathbf{C} \mathbf{w}$ can be written $w_1^2 \Delta C_{11} + w_2^2 \Delta C_{22} + \dots + w_S^2 \Delta C_{SS}$, so we have

$$\alpha_1 \approx (\beta_1 + \mu_d) + \sum_{i=1}^S w_i^2 \Delta C_{ii}. \quad (\text{B34})$$

Therefore, maximizing/minimizing α_1 is equivalent to maximizing/minimizing the sum on the right hand side. The coefficients w_i^2 are always nonnegative while the C_{ii} are both negative and positive

(since they are the deviations from the mean intraspecific interaction strength). Maximization (minimization) of the sum is therefore achieved by pairing up large values of w_i^2 with large (small) entries of ΔC_{ii} , and small values of w_i^2 with small (large) entries of ΔC_{ii} .

In the maximum β_1 case (1. and 2. above), species are sorted in increasing order of the components of the eigenvector \mathbf{w} corresponding to the rightmost eigenvalue β_1 of \mathbf{B} . It is therefore both the vector corresponding to the eigenvalue to be perturbed and also the one based on which the species are ordered. Due to this fact, we have $w_1 \leq w_2 \leq \dots \leq w_S$. Note that \mathbf{w} is the eigenvector belonging to the rightmost and not the dominant eigenvalue; and since only the dominant eigenvector can have components with all the same sign, \mathbf{w} will necessarily have both positive and negative components (a simple corollary of the Perron–Frobenius theorem). Because of this, it is *not* true that $w_1^2 \leq w_2^2 \leq \dots \leq w_S^2$. Instead, the w_i^2 first decrease, then increase as i runs from 1 to S , forming a V-shape (Figure B5, top row). Then, to maximize α_1 , the largest ΔC_{ii} should be paired with the largest w_i^2 , leading to a diagonal that also follows a V-shape—which is precisely what we see in the cases of maximizing α_1 with either a random or maximal β_1 . In turn, α_1 is minimized when the smallest ΔC_{ii} are paired up with the largest w_i^2 , leading to the upside-down V-shape.

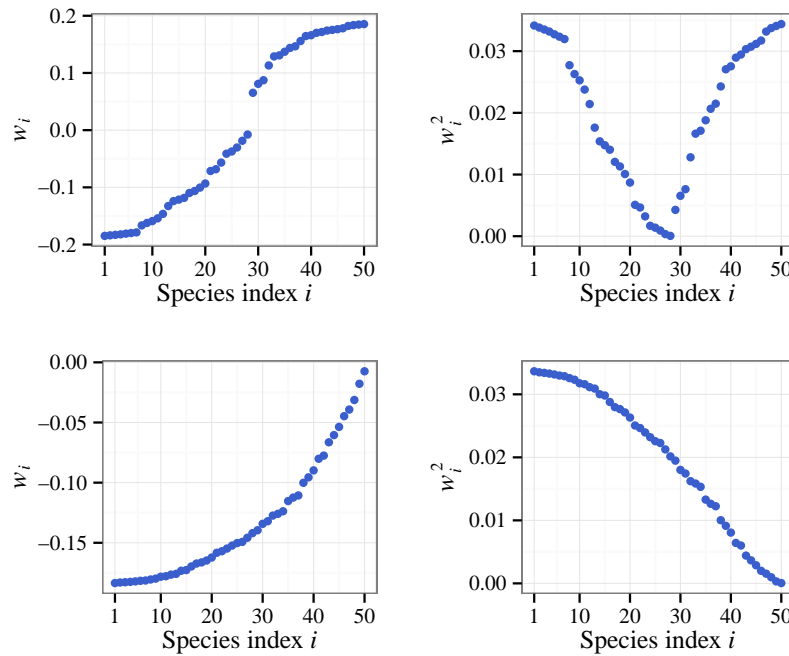


Figure B5: Eigenvectors’ components sorted in increasing order, and the squared components in that same order. Top: the leading eigenvector has both negative and positive entries. The squared components will therefore first decrease, then increase. Bottom: the dominant eigenvector can be chosen all-negative by the Perron–Frobenius theorem. Its squared components therefore monotonically decrease.

We still see these arrangements in the random cases (3. and 4. above), though they are less pronounced than in the maximum β_1 case. Since the matrix \mathbf{B} is random, one might wonder why we see a pattern at all. The reason is that species are still ordered based on the leading eigenvector. Therefore, despite the randomness, matrix entries tend to increase towards the upper-right and

lower-left corners of the matrices, though this increase is no longer strictly monotonic. This means that the broad pattern is retained, but it is expected to be fuzzier than before, which is exactly what we see.

Finally, in the minimum β_1 cases (5. and 6. above), species are ordered not by the leading but by the dominant eigenvector (i.e., the one belonging to the eigenvalue that is largest in magnitude, not in value). Since the matrix \mathbf{A} is negative, the Perron–Frobenius theorem applies to $-\mathbf{A}$, and so the leading eigenvector can be chose to have all negative components. When ordering species based on it, we have $w_1 \leq w_2 \leq \dots \leq w_S$, and since all w_i are negative, it follows that $w_1^2 \geq w_2^2 \geq \dots \geq w_S^2$ (Figure B5, bottom row). Therefore, were our goal to maximize (minimize) this eigenvalue instead of the leading one, ΔC_{ii} would have to be arranged in decreasing (increasing) order. When maximizing/minimizing the dominant eigenvalue, keep in mind that the mean and the variance of \mathbf{A} 's eigenvalue distribution does not change by swapping diagonal entries. Therefore, maximizing (minimizing) this eigenvalue will cause all the other $S - 1$ eigenvalues to a) shift very slightly in the negative (positive) direction to retain the mean, and b) to reduce (increase) their spread to retain the variance. The shift in the mean is going to be negligible for S sufficiently large, therefore the change in the spread of the $S - 1$ other eigenvalues will determine whether the leading (not the dominant!) eigenvalue will increase or decrease. It decreases when their spread decreases, and vice versa. Therefore, minimizing the dominant eigenvalue is expected to also minimize the leading eigenvalue, and conversely, maximizing the leading eigenvalue will maximize the dominant one, leading to the observed patterns.

In the random and minimum β_1 cases, there is an extra complication when minimizing α_1 . Since many eigenvalues have very similar values, minimizing the leading eigenvalue may cause it to cross other eigenvalues. It therefore ceases to be the leading eigenvalue. To truly minimize the rightmost eigenvalue, an appropriate linear combination of eigenvectors must be considered, which may confound the simple patterns described above. This is seen in Figure 1 of the main text: for minimum β_1 and α_1 , the decrease in the magnitude of interaction strengths is not quite monotonic.

As a final note, the argument of this section relied on the linear eigenvalue perturbation formula, Eq. (B33). Thus, one expects it to hold if the entries of the perturbing matrix $\Delta \mathbf{C}$ are not too large in magnitude compared to those of $\mathbf{B} + \mu_d \mathbf{I}$. Deviations from the expected pattern may happen if $\Delta \mathbf{C}$ has very strong entries, i.e., if the diagonal variance V_d is too large. However, even in those cases, the general shapes predicted by our argument hold up (see the Supplementary Figures S1–S20).

B7 Calculating the domain of feasibility

The coexistence equilibrium $\hat{\mathbf{n}} = -\mathbf{A}^{-1}\mathbf{b}$ of the Lotka–Volterra model is feasible if all equilibrium densities are positive (Section B1). For a given interaction matrix \mathbf{A} , the direction of \mathbf{b} determines feasibility but not its magnitude, because if $\hat{\mathbf{n}} = -\mathbf{A}^{-1}\mathbf{b} > \mathbf{0}$, then so is $\eta\hat{\mathbf{n}} = -\mathbf{A}^{-1}(\eta\mathbf{b})$ for an arbitrary positive constant η (Section B2). To evaluate feasibility, we can therefore determine the number of directions of \mathbf{b} that lead to a feasible solution, out of all possible directions. We call this quantity Ξ :

$$\Xi = \frac{(\text{number of directions of } \mathbf{b} \text{ leading to a feasible coexistence equilibrium})}{(\text{all possible directions of } \mathbf{b} \text{ in the positive orthant})}. \quad (\text{B35})$$

Restricting the possible directions of \mathbf{b} to the positive orthant is equivalent to assuming that all intrinsic growth rates are positive. Since the system is competitive, no coexistence is possible

without this assumption in the first place. One can evaluate Ξ analytically for two (Section B2.2) and three (Svirezhev and Logofet 1983, pp. 203–204) species. For more than three species, no known closed-form solutions exist. In lieu of an analytical formula, Grilli et al. (2015) provide an accurate and efficient method for calculating Ξ by numerically evaluating the integral

$$\Xi = \frac{2^S \Gamma(S/2) |\det(\mathbf{A})|}{2\pi^{S/2}} \int_{\Omega^+} \left(\sum_{i=1}^S \sum_{j=1}^S \sum_{k=1}^S b_i A_{ki} A_{kj} b_j \right)^{-S/2} db_1 db_2 \cdots db_S. \quad (\text{B36})$$

Here S is the number of species, $\Gamma(\cdot)$ is the Gamma function, $\det(\mathbf{A})$ is \mathbf{A} 's determinant, Ω^+ is the part of the S -dimensional unit sphere's surface that falls in the positive orthant, b_1, \dots, b_S are the components of \mathbf{b} normalized so that the vector has length 1 (i.e., \mathbf{b} always lies on the unit sphere's surface within the positive orthant), and A_{ij} is the (i, j) th entry of \mathbf{A} . To obtain our feasibility results, we numerically evaluated this integral via the Monte Carlo method.

An increasing number of species S has a trivial dimensional effect on the fraction of feasible directions Ξ . If half the total angle per direction in an S -species system is feasible, then by Eq. (B35) we get $\Xi = 2^{-S}$. But, although the total fraction of feasible directions is decreasing, the fraction of feasible directions *per dimension* stays the same, $1/2$. For this reason, we use $\sqrt[S]{\Xi}$ instead of Ξ to quantify feasibility, which is a measure of the (geometric) average fraction of feasible directions per dimension. It also has the advantage of allowing for the comparison of systems with different numbers of species S .

References from the Appendices

- Allesina, S., and S. Tang. 2015. The stability-complexity relationship at age 40: a random matrix perspective. *Population Ecology* 57:63–75.
- Bai, Z., and J. W. Silverstein. 2009. Spectral analysis of large dimensional random matrices. Springer.
- Caswell, H. 2001. Matrix population models: Construction, analysis, and interpretation. 2nd edition. Sinauer Associates.
- Chesson, P. 2000. Mechanisms of maintenance of species diversity. *Annual Review of Ecology and Systematics* 31:343–366.
- Grilli, J., M. Adorisio, S. Suweis, G. Barabás, J. R. Banavar, S. Allesina, and A. Maritan. 2015. The geometry of coexistence in large ecosystems pages arXiv:1507.05337 [q-bio.PE].
- Hernández-García, E., C. López, S. Pigolotti, and K. H. Andersen. 2009. Species competition: coexistence, exclusion and clustering. *Philosophical Transactions of the Royal Society London, Series A* 367:3183–3195.
- Hofbauer, J., and K. Sigmund. 1988. The Theory of Evolution and Dynamical Systems. Cambridge University Press, Cambridge.
- Horn, R., and C. R. Johnson. 2012. Matrix Analysis. Cambridge University Press, Cambridge.

- MacArthur, R. H. 1970. Species packing and competitive equilibria for many species. *Theoretical Population Biology* 1:1–11.
- Mallet, J. 2012. The struggle for existence: how the notion of carrying capacity, K , obscures the links between demography, Darwinian evolution, and speciation. *Evolutionary Ecology Research* 14:627–665.
- May, R. M., and W. J. Leonard. 1975. Nonlinear aspects of competition between three species. *SIAM Journal on Applied Mathematics* 29:243–253.
- McGill, B. J., R. S. Etienne, J. S. Gray, D. Alonso, M. J. Anderson, H. K. Benecha, M. Dornelas, B. J. Enquist, J. L. Green, F. He, A. H. Hurlbert, A. E. Magurran, P. A. Marquet, B. A. Maurer, A. Ostling, C. U. Soykan, K. I. Ugland, and E. P. White. 2007. Species abundance distributions: moving beyond single prediction theories to integration within an ecological framework. *Ecology Letters* 10:995–1015.
- O’Rourke, S., and D. Renfrew. 2014. Low rank perturbations of large elliptic random matrices. *Electronic Journal of Probability* 19:1–65.
- Smale, S. 1976. On the differential equations of species in competition. *Journal of Mathematical Biology* 3:5–7.
- Sommers, H. J., A. Crisanti, H. Sompolinsky, and Y. Stein. 1998. Spectrum of large random asymmetric matrices. *Physical Review Letters* 60:1895–1898.
- Svirezhev, Y. M., and D. O. Logofet. 1983. *Stability of Biological Communities*. Mir Publishers, Moscow, Russia.
- Tokita, K. 2004. Species abundance patterns in complex evolutionary dynamics. *Physical Review Letters* 93:178102.
- Vandermeer, J. H. 1975. Interspecific competition: A new approach to the classical theory. *Science* 188:253–255.
- Vano, J. A., J. C. Wildenberg, M. B. Anderson, J. K. Noel, and J. C. Sprott. 2006. Chaos in low-dimensional Lotka–Volterra models of competition. *Nonlinearity* 19:2391–2404.
- Yoshino, Y., T. Galla, and K. Tokita. 2008. Rank abundance relations in evolutionary dynamics of random replicators pages arXiv:0803.1082v2 [q-bio.PE].
- Zeeman, M. L. 1993. Hopf bifurcations in competitive three-dimensional Lotka–Volterra systems. *Dynamics and Stability of Systems* 8:189–216.

Supplementary Figures

The figures below (Figures S1–S20) show that the results reported in the main text are robust across various parameterizations. The first three of each parameterization read exactly like Figures 1–3 in the main text, except for the set of intra- and interspecific coefficients, which we report in the figure captions. The additional two figures of each parameterization show the relationship of the leading eigenvalue of the most/least stabilized configuration of coefficients with respect to a distribution generated by randomly assorting those coefficients.

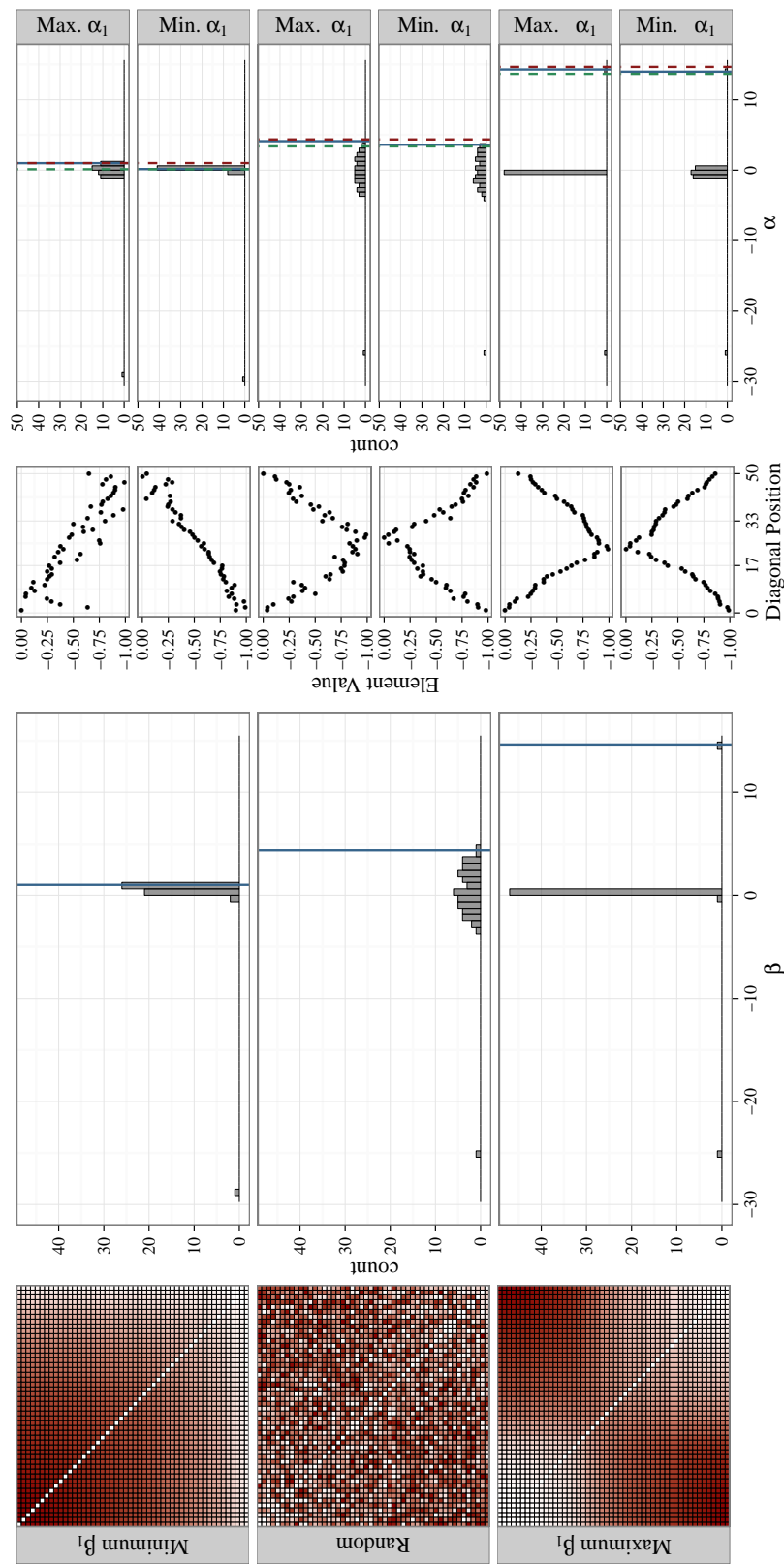


Figure S1: As Figure 1 in the main text, except the interspecific competition coefficients are uniformly sampled from $[-1, 0]$, and the intraspecific coefficients are also uniformly sampled from $[-1, 0]$.

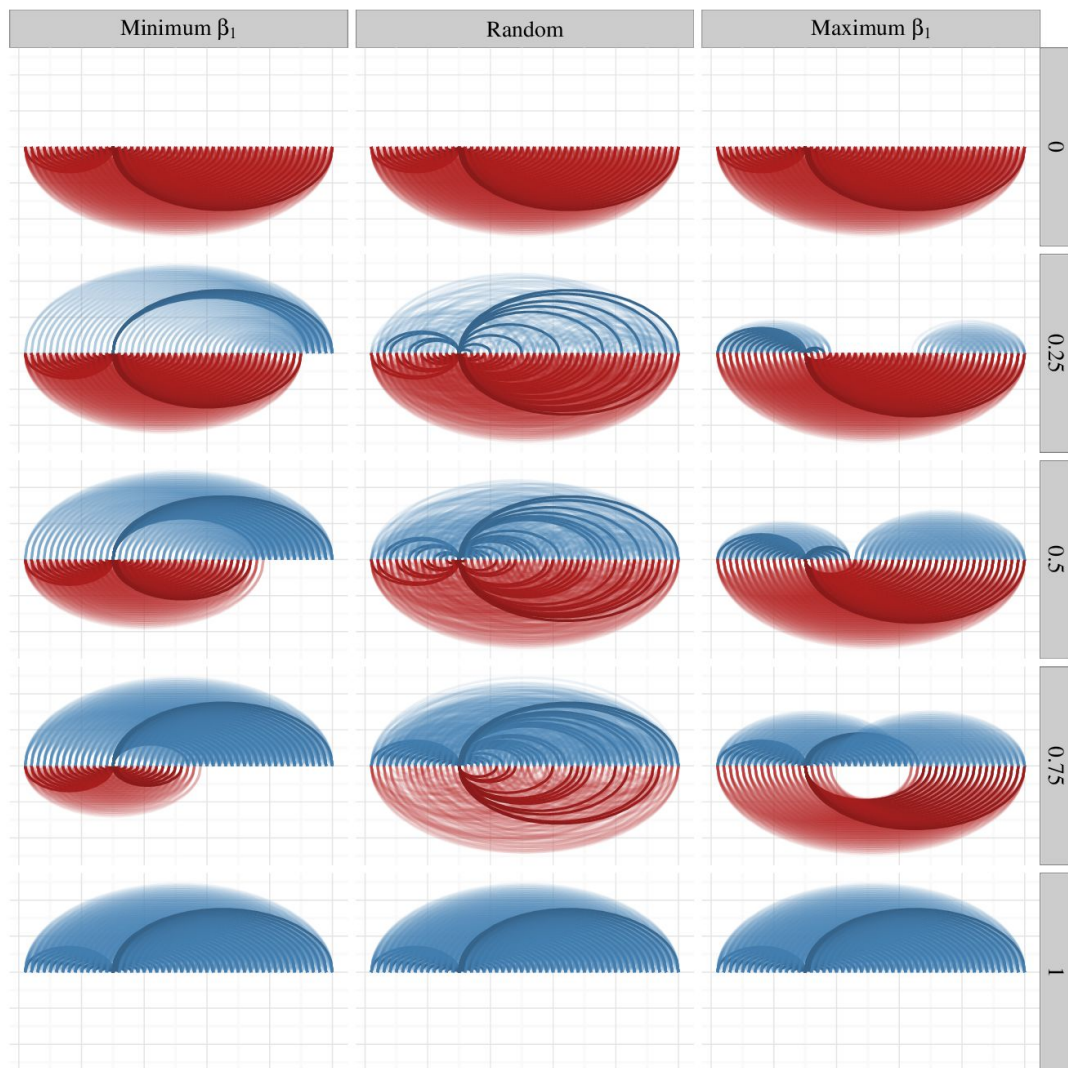


Figure S2: As Figure 2 in the main text, except with the three interspecific interaction matrices in Figure S1.

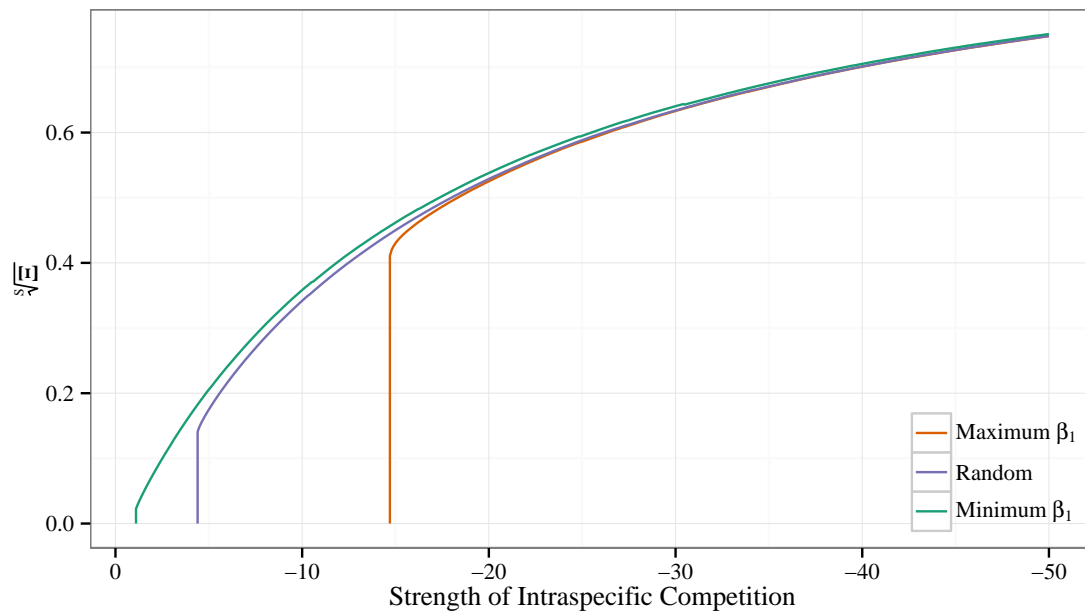


Figure S3: As Figure 3 in the main text, except the interspecific competition coefficients are uniformly sampled from $[-1, 0]$.

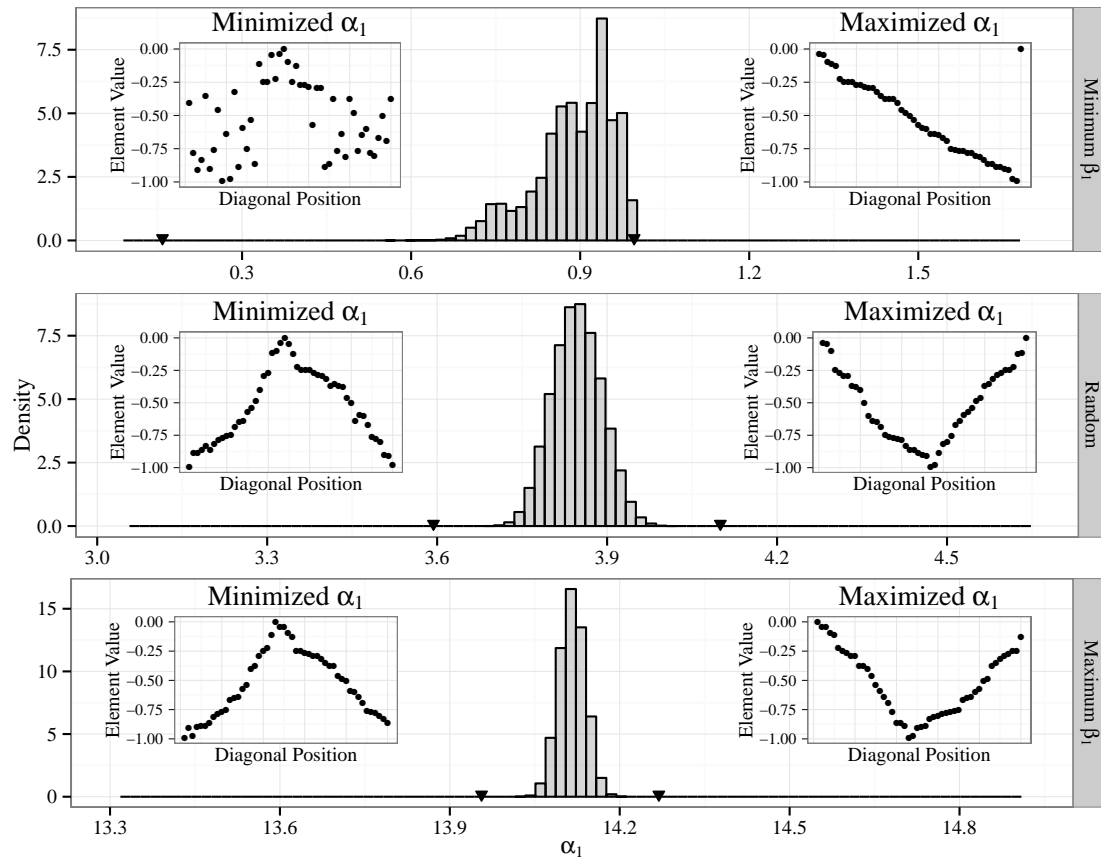


Figure S4: Distributions of the rightmost eigenvalue α_1 of $\mathbf{A} = \mathbf{B} + \mathbf{C}$ (\mathbf{B} contains only interspecific, \mathbf{C} only intraspecific effects) in a 50-species community, when the rightmost eigenvalue β_1 of \mathbf{B} is minimized (top), corresponds to a random matrix (middle), or maximized (bottom). The histogram in each row is generated by 100,000 random permutations of \mathbf{C} 's diagonal coefficients. Species in the insets are ordered as in Figure S1. In each of the three cases, we also looked for the particular arrangement which minimizes/maximizes α_1 , using a genetic optimization algorithm (left/right insets showing the magnitudes of \mathbf{C} 's diagonal entries in order; their corresponding values of α_1 are marked by the arrows). Interspecific competition coefficients are uniformly sampled from $[-1, 0]$, and the intraspecific coefficients are also uniformly sampled from $[-1, 0]$.

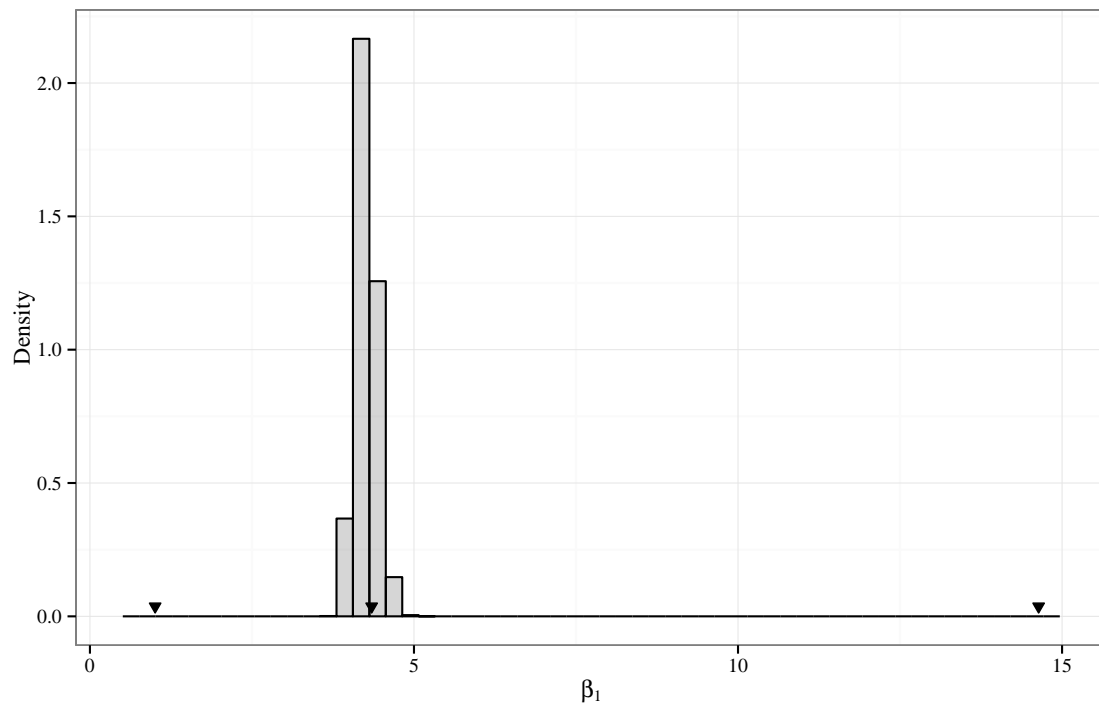


Figure S5: Distributions of the rightmost eigenvalue β_1 of \mathbf{B} in a 50-species community. The histogram is generated by 100,000 random permutations of \mathbf{B} 's coefficients. The black arrows indicate the rightmost eigenvalues of the most stabilized, random, and least stabilized configurations, respectively (as in Figure S1). The first and last of which were found using a genetic optimization algorithm. The most stabilized matrix has been sorted according to the eigenvector associated with the left-most eigenvalue; the other two are sorted by the eigenvector associated with the right-most eigenvalue. Interspecific competition coefficients are uniformly sampled from $[-1, 0]$.

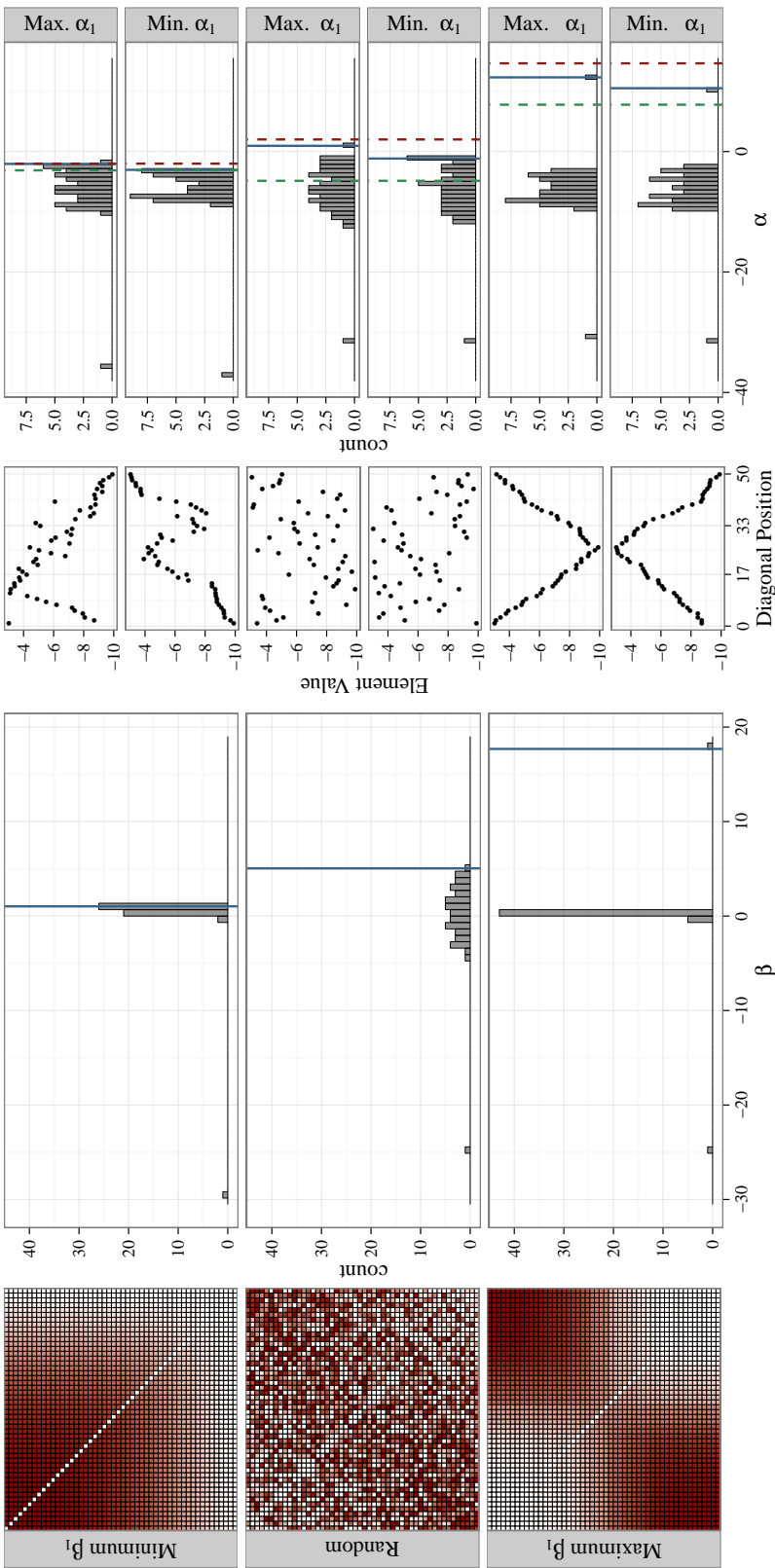


Figure S6: As Figure 1 in the main text, except the interspecific competition coefficients are sampled from a beta distribution with parameters $(1/2, 1/2)$, and the intraspecific coefficients are uniformly sampled from $[-10, -3]$.

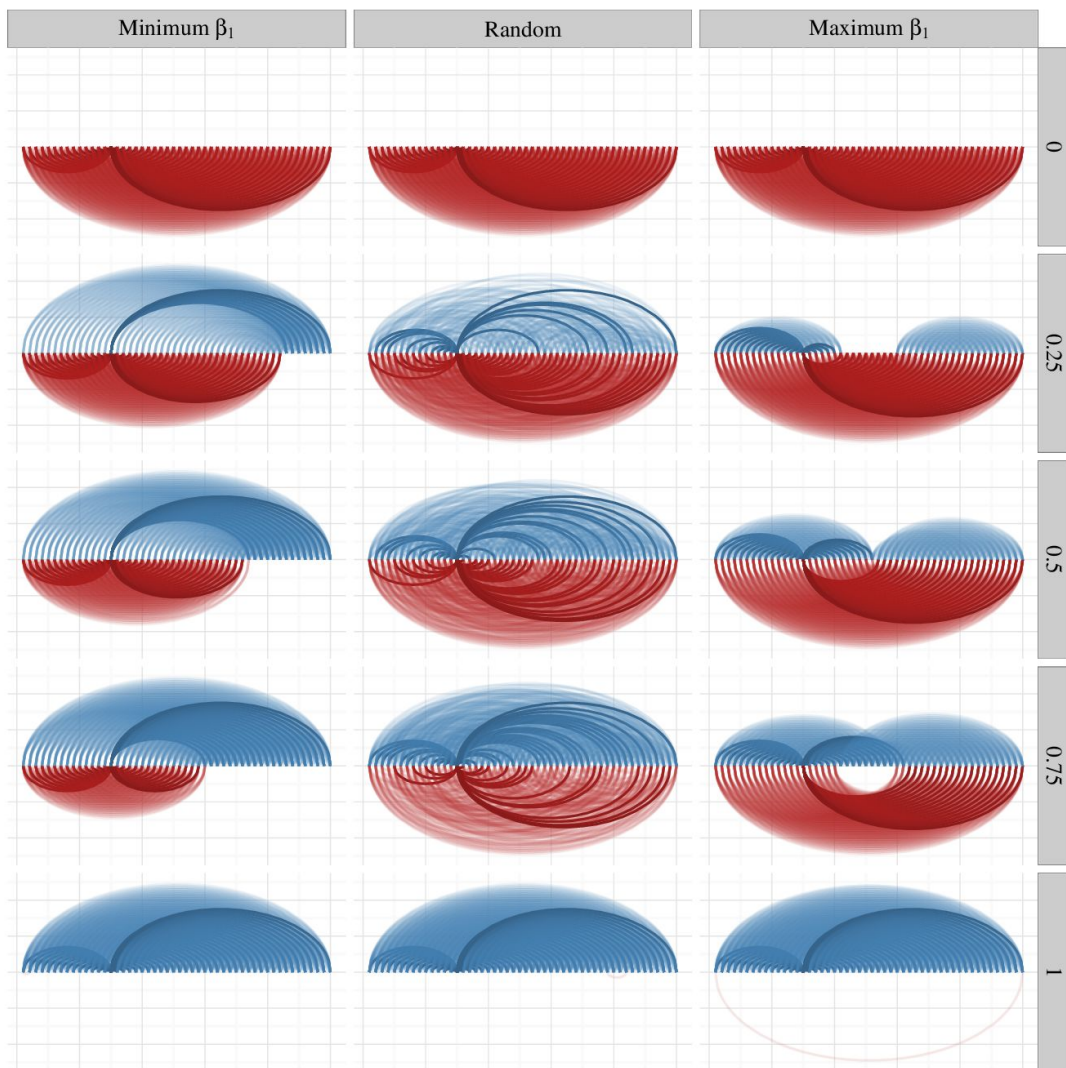


Figure S7: As Figure 2 in the main text, except with the three interspecific interaction matrices in Figure S6.

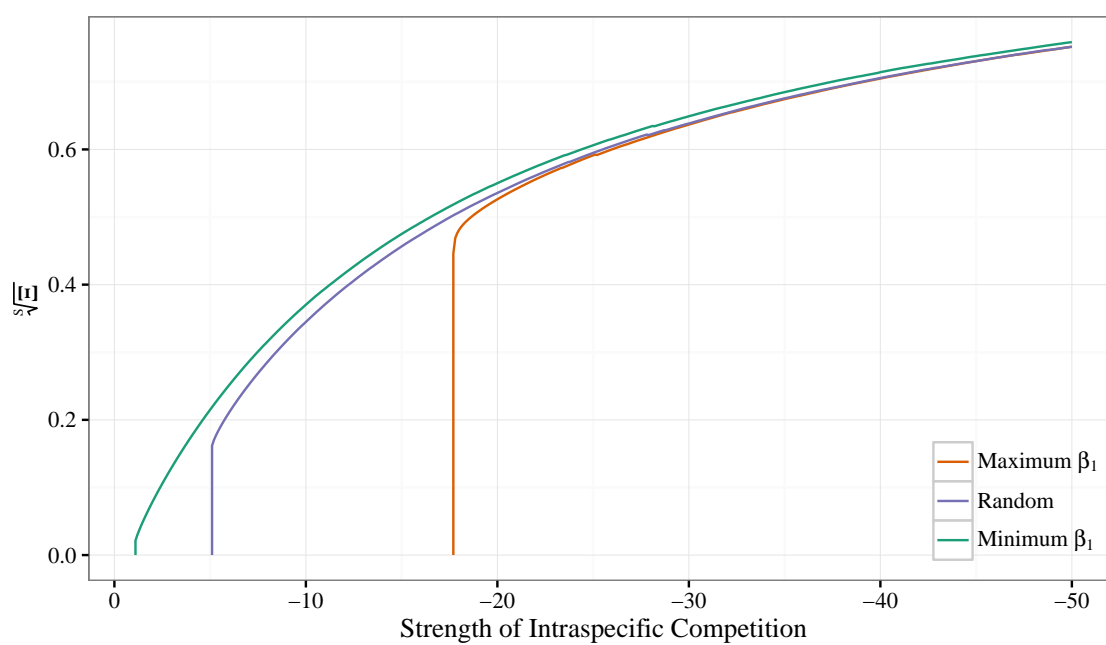


Figure S8: As Figure 3 in the main text, except the interspecific competition coefficients are sampled from a beta distribution with parameters $(1/2, 1/2)$.

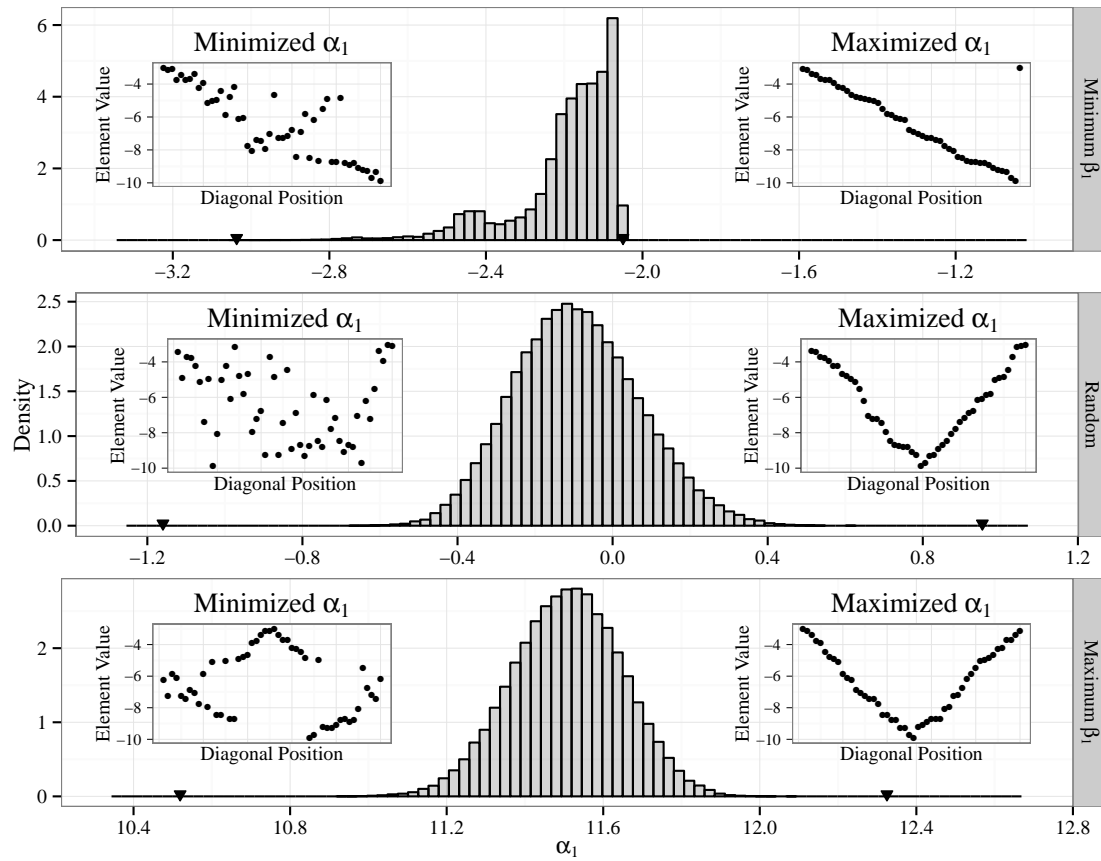


Figure S9: As Figure S4, except with interspecific competition coefficients are uniformly sampled from $[-1, 0]$, and the intraspecific coefficients are also uniformly sampled from $[-1, 0]$.

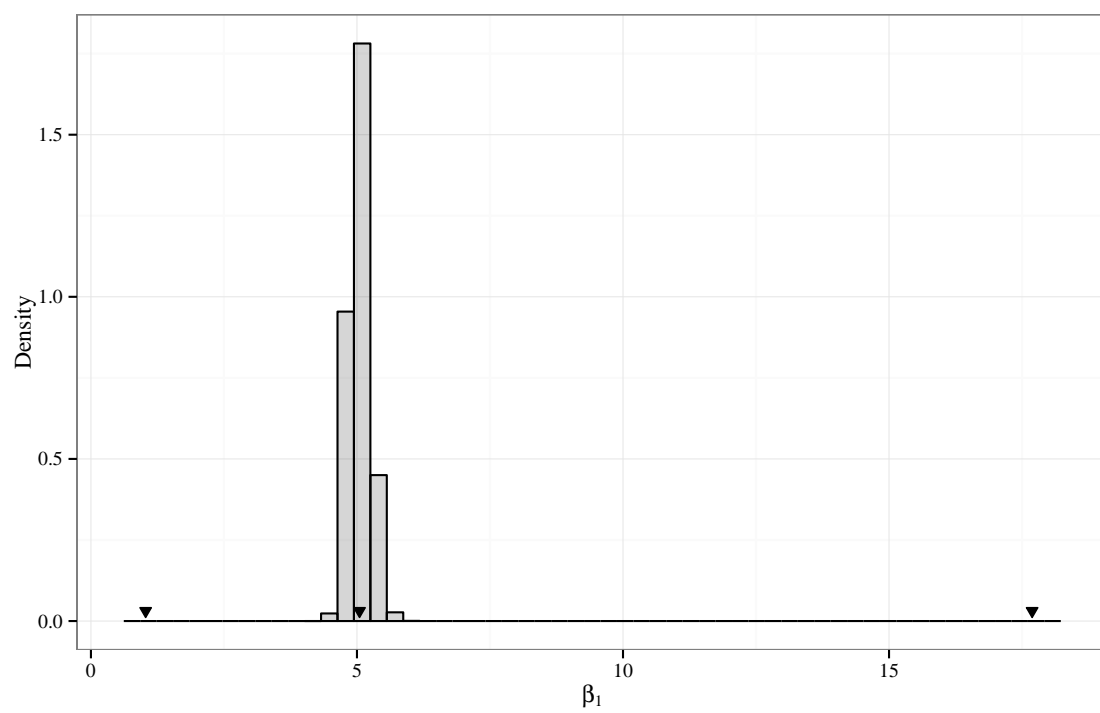


Figure S10: As Figure S5, except with interspecific competition coefficients are uniformly sampled from $[-1, 0]$.

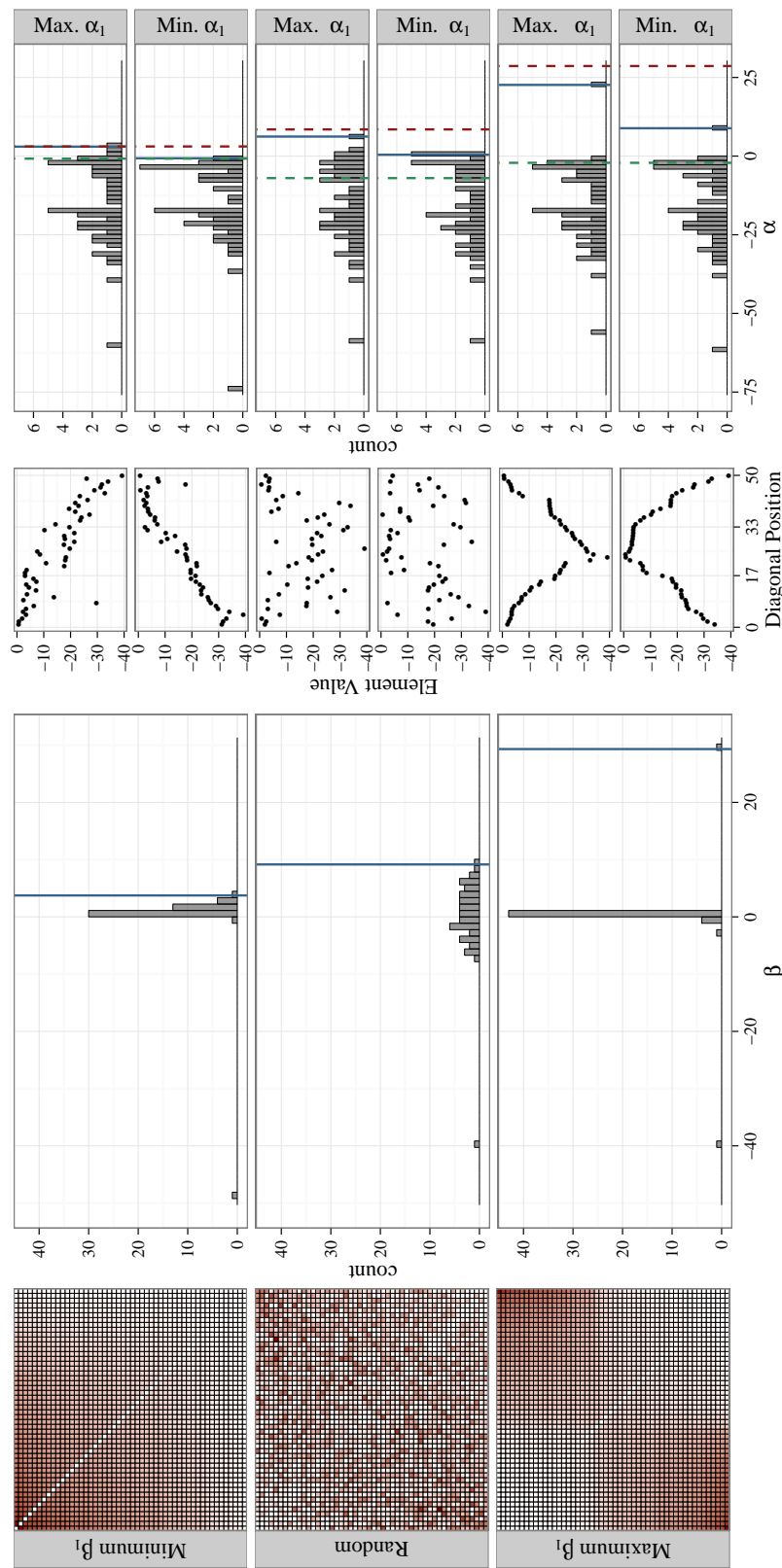


Figure S11: As Figure 1 in the main text, except the interspecific competition coefficients are sampled from a half-normal distribution with $\sigma = 1$, and the intraspecific coefficients are sampled from a half-normal distribution with $\sigma = 20$.

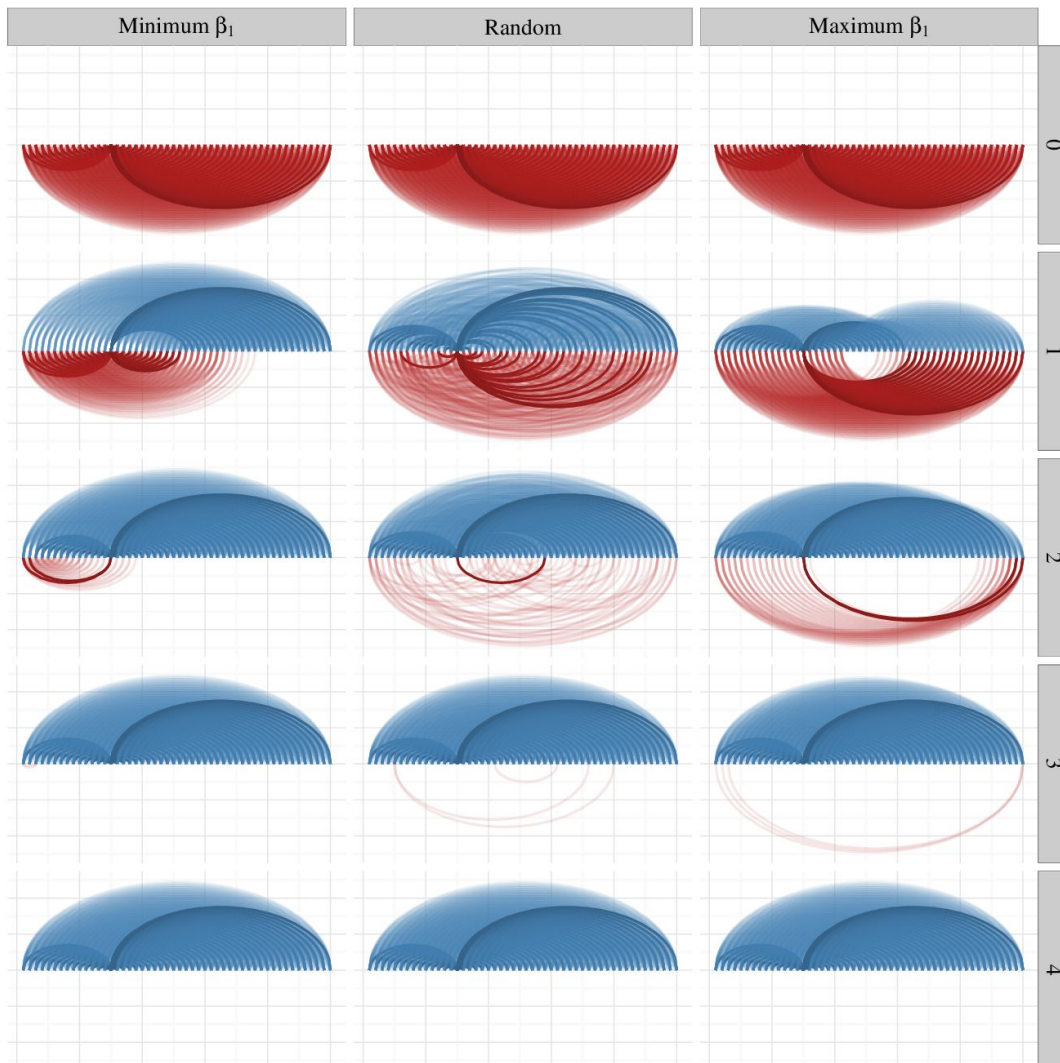


Figure S12: As Figure 2 in the main text, except with the three interspecific interaction matrices in Figure S11.

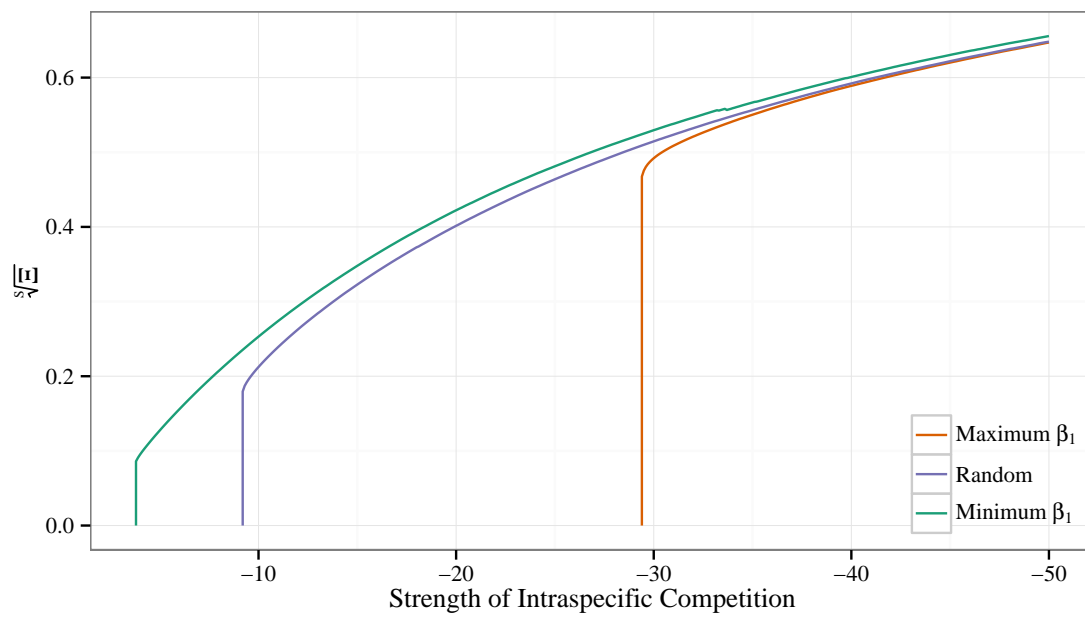


Figure S13: As Figure 3 in the main text, except the interspecific competition coefficients are sampled from a half-normal distribution with $\sigma = 1$.

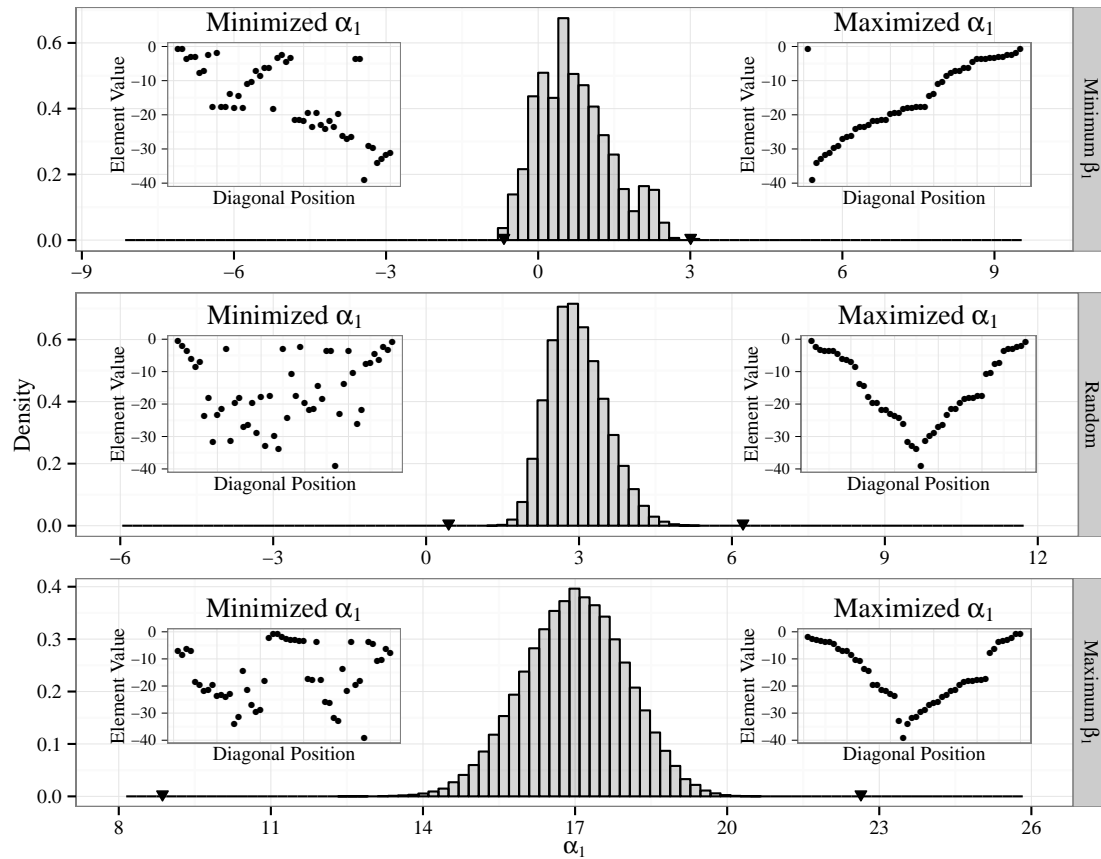


Figure S14: As Figure S4, except with interspecific competition coefficients are uniformly sampled from $[-1, 0]$, and the intraspecific coefficients are also uniformly sampled from $[-1, 0]$.

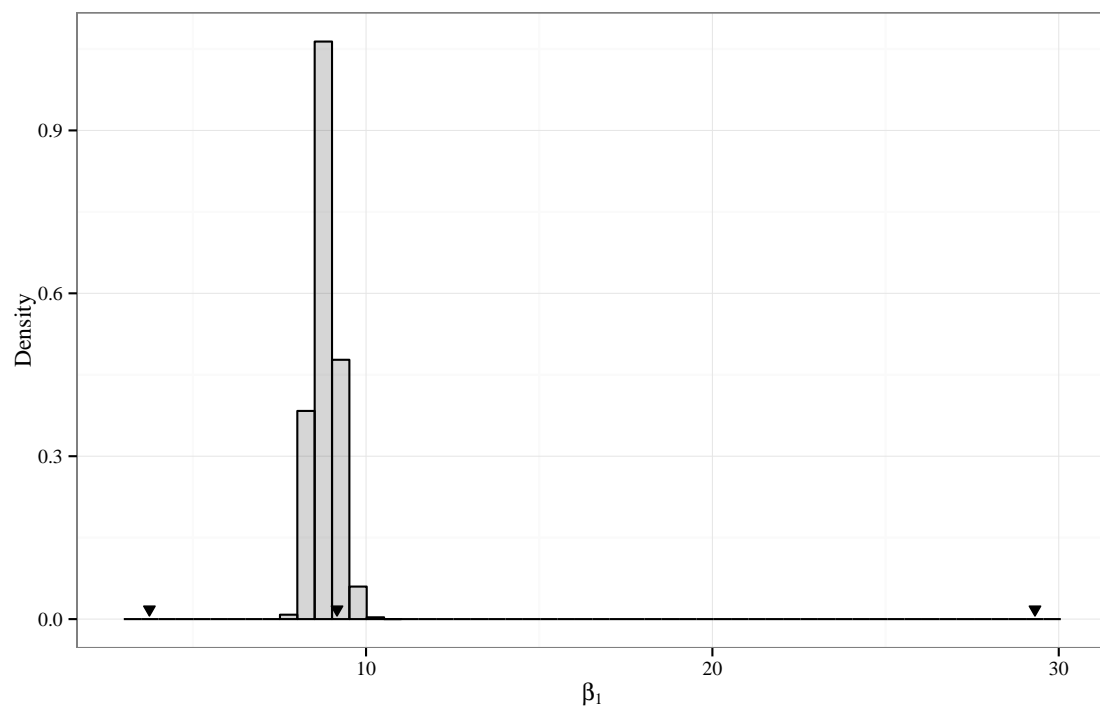


Figure S15: As Figure S5, except the interspecific competition coefficients are sampled from a half-normal distribution with $\sigma = 1$, and the intraspecific coefficients are sampled from a half-normal distribution with $\sigma = 20$.

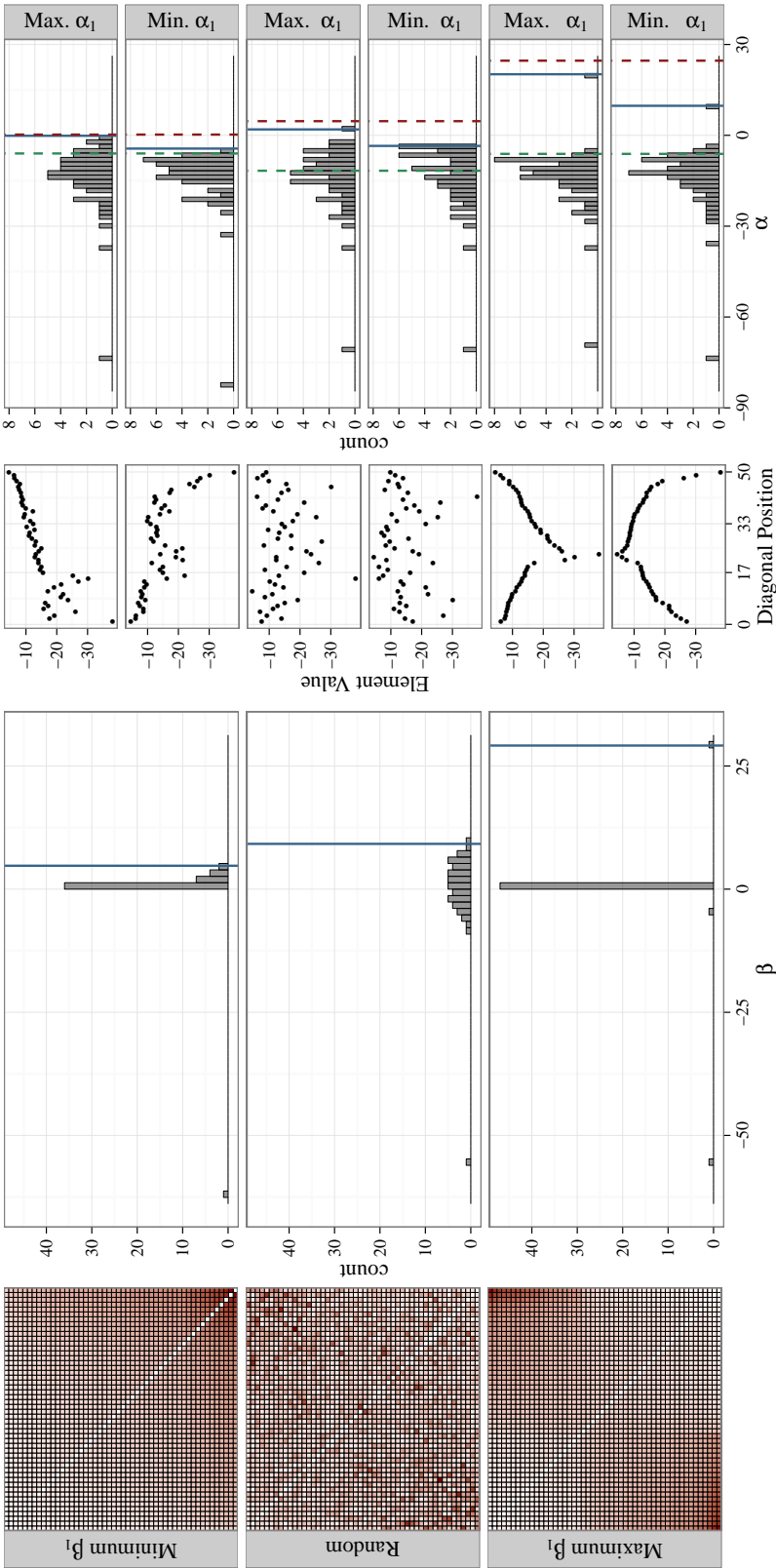


Figure S16: As Figure 1 in the main text, except the interspecific competition coefficients are sampled from a lognormal distribution with parameters $\mu = 0$, $\sigma = 0.5$, and the intraspecific coefficients are sampled from a lognormal distribution with parameters $\mu = 2.5$, $\sigma = 0.5$.

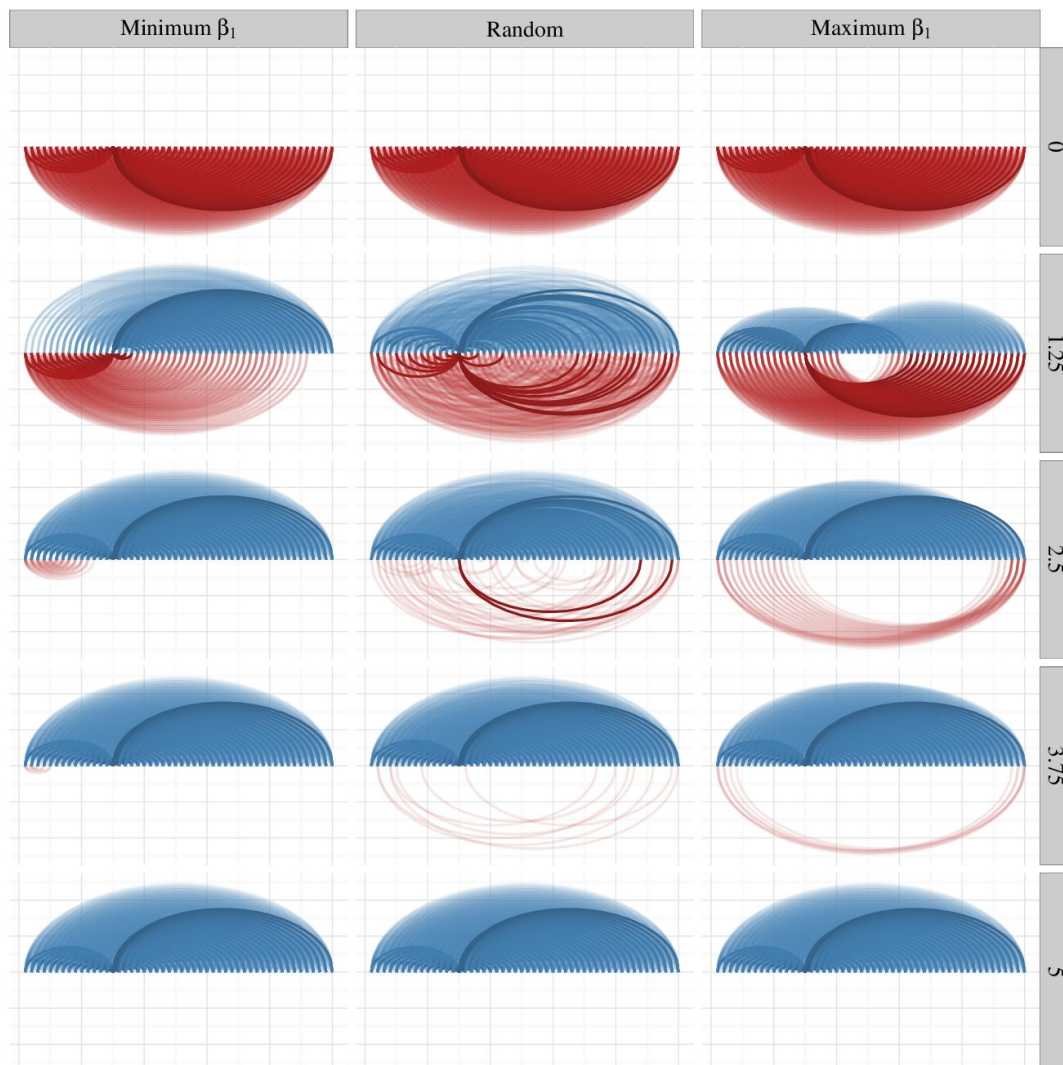


Figure S17: As Figure 2 in the main text, except with the three interspecific interaction matrices in Figure S16.

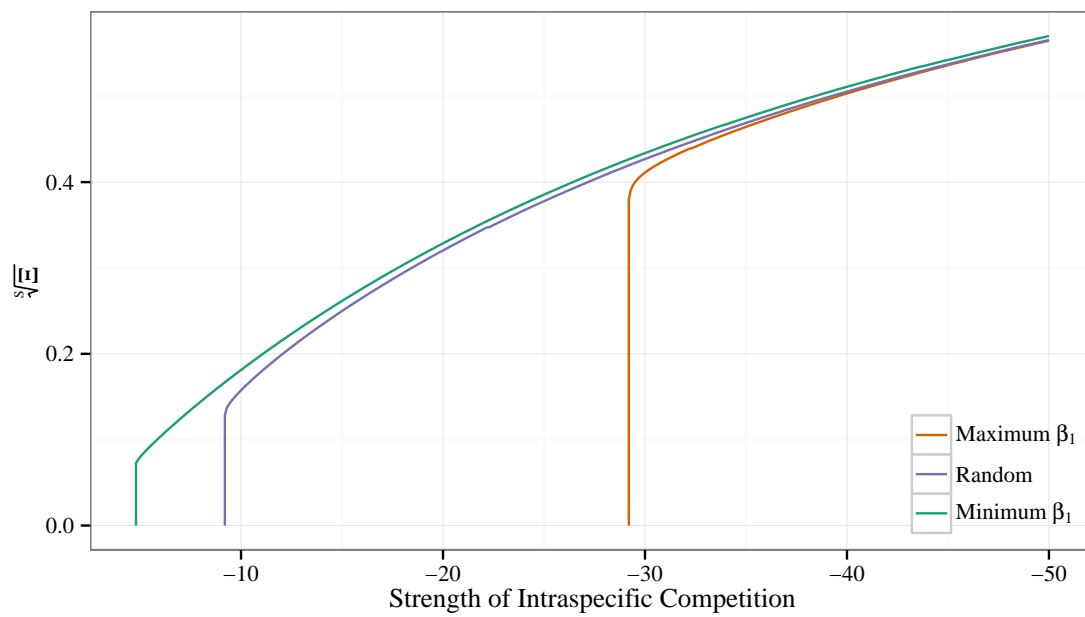


Figure S18: As Figure 3 in the main text, except the interspecific competition coefficients are sampled from a lognormal distribution with parameters $\mu = 0$, $\sigma = 0.5$.

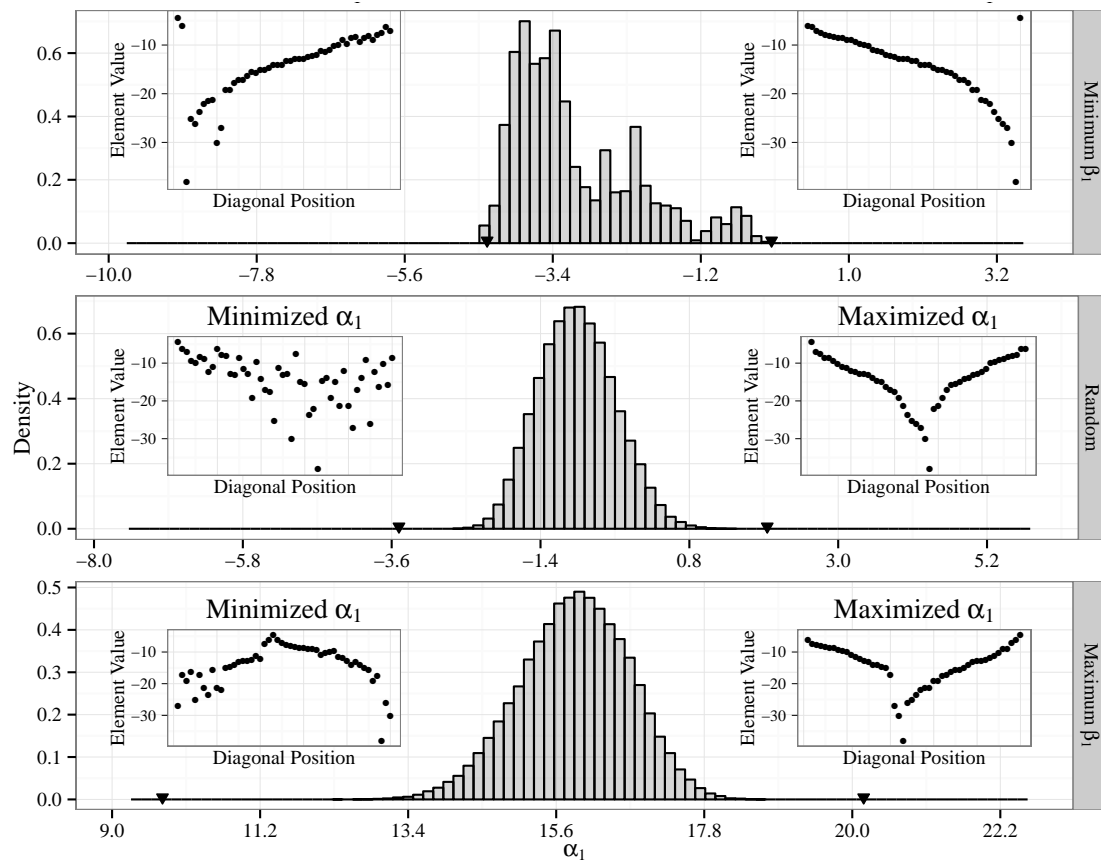


Figure S19: As Figure S4, except the interspecific competition coefficients are sampled from a lognormal distribution with parameters $\mu = 0$, $\sigma = 0.5$, and the intraspecific coefficients are sampled from a lognormal distribution with parameters $\mu = 2.5$, $\sigma = 0.5$.

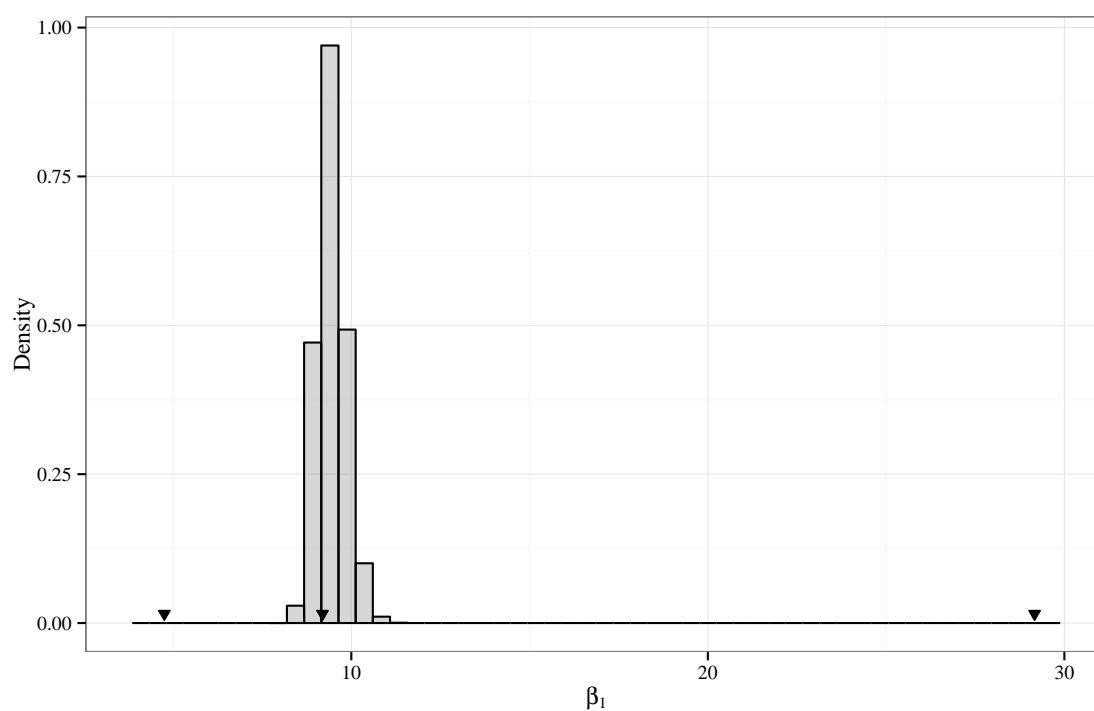


Figure S20: As Figure S5, except the interspecific competition coefficients are sampled from a lognormal distribution with parameters $\mu = 0$, $\sigma = 0.5$.